UDK/UDC: 621.791 **ISSN 0354-7965**

ZAVARIVANJE I ZAVARENE KONSTRUKCIJE

WELDING & WELDED STRUCTURES

God. 64	Br. 4	145-192	Beograd	Srbija	2019.
Vol. 64	No. 4	145-192	Belgrade	Serbia	2019.

ČASOPIS DRUŠTVA ZA UNAPREĐIVANJE ZAVARIVANJA U SRBIJI

SERBIAN WELDING SOCIETY QUARTERLY REVIEW

IZLAZI TROMESEČNO

CIP - Каталогизација у публикацији
Народна библиотека Србије, Београд

621.791

ZAVARIVANJE i zavarene konstrukcije : časopis Društva za unapređivanje zavarivanja u Srbiji = Welding & Welded Structures : Serbian Welding Society quarterly review / glavni i odgovorni urednik = editor-in-chief Milica Antić. – Vol. 41, no. 1 (1996)- . - Beograd : Društvo za unapređivanje zavarivanja u Srbiji, 1996-. (Beograd : VIS studio).-29 cm

Tromesečno.
ISSN 0354-7965 = Zavarivanje i zavarene konstrukcije
COBISS.SR-ID 105396743

CENE I NARUDŽBINA ZA 2019.

Cena pojedinačnog broja 825,00 dinara

Godišnja pretplata 2500,00 dinara

Tekući račun: 325-9500600002588-46

PRICE AND ORDER

Annual subscription: EUR 100

Account No. RS35325960160000041546

OTPVRS22 (VOJVOĐANSKA BANKA AD)

IBAN RS35325960160000041546

ŠTAMPA / PRINTED

"VIS STUDIO" d.o.o.
Aleksinačkih rudara 35, Beograd
Tiraž: 400 kom.

Časopis sufinansira Ministarstvo prosvete, nauke i tehnološkog razvoja Republike Srbije

Na osnovu mišljenja Ministarstva za nauku, tehnologije i razvoj Republike Srbije br. 413-00-2272/2001-01, časopis ZAVARIVANJE I ZAVARENE KONSTRUKCIJE je publikacija od posebnog interesa za nauku

4/2019

SADRŽAJ CONTENTS

Dragi moji,

svi mi obasuti ili dodirnuti, opečeni ili obasjani vatrom zavarivanja, posvećeni knjizi, izmučeni električnim lukom, opčinjeni ili zdrobljeni organizacijom, u istom smo krugu. Svako od nas na različitom mestu.

Utičemo li na to ili umišljamo? Da li uspevamo ili mislimo da smo već uspeli? Da li nas novo jutro guši ili veseli? Da li nas posao zadovoljava ili zarobljava? Da li je novac blagodet ili prokletstvo?

Ciljevi nam nisu isti. Ma koliko oni bili različiti, još su različitiji načini stizanja do njih. Sve što smo učinili ili nismo učinili, čeka nas, ponekad u zasedi, ponekad iščekujemo.

Svi smo samo ljudi a zajednički sudija nam je VREME.

Želimo vam da u novoj godini budete srećni i uspešni. Neka u nastupajućoj prestupnoj godini nas i naših okupljanja bude više. Zdravi bili.

Glavni i odgovorni urednik
Milica Antić, dipl.ing, EWE

<u>Podsećamo vas da je sada vreme da obnovite vaše članstvo u DUZS i pretplatu za naš časopis.</u>

METALURGIJA ZAVARIVANJA

Radica Prokić Cvetković, Olivera Popović

Prava je prilika da ovu publikaciju izašlu iz štampe krajem oktobra ove godine, predstavimo našem čitalaštvu.

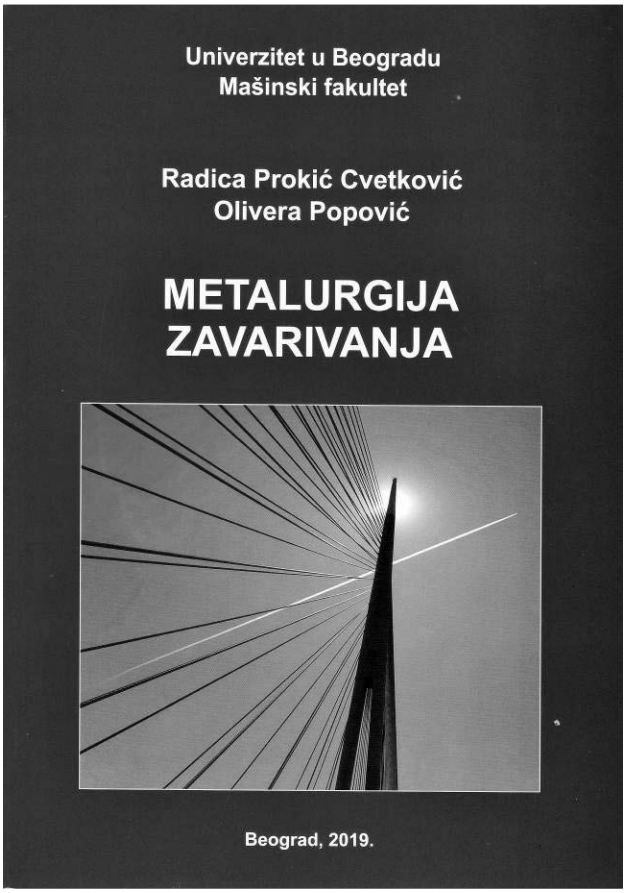

Ovaj udžbenik nastao iz potreba obrazovanja studenata Mašinskog fakulteta u Beogradu, uveliko prevazilazi svoju namenu. Radi boljeg uvida poslužiće deo predgovora:

„*U želji da preglednije i jednostavnije predstave ovako kompleksnu materiju, autori su odlučili da je izlože kroz sledeća poglavlja: osnovni pojmovi u zavarivanju, toplotni procesi pri zavarivanju, naponi i deformacije u zavarenim spojevima, hemijske reakcije pri zavarivanju, strukturne promene u zavarenim spojevima, zavarljivost, termička obrada zavarenih spojeva, čelici, podela i označavanje čelika, zavarivanje nelegiranih čelika, zavarivanje čelika visoke čvrstoće, zavarivanje čelika za rad na niskim temperaturama, zavarivanje čelika otpornih na puzanje, zavarivanje nerđajućih čelika, zavarivanje raznorodnih materijala, zavarivanje gvožđa, zavarivanje aluminijuma i njegovih legura, zavarivanje bakra, nikla i njihovih legura, zavarivanje titana i ostalih obojenih metala, zavarivanje polimera, keramike i kompozita.*“

Iz pregleda sadržaja jasno je da ovakav materijal u vrlo velikom stepenu, odgovara polaznicima kurseva za međunarodne inženjere i tehnologe, a odličan je alat za one koji se dugo bave samo po nekim grupama čelika u trenutku kada treba da rešavju probleme zavarivanja nekih „novih“, a i dobar podsetnik za nas koji „sve znamo“.

Ovakvu knjigu bi trebalo da ima svako ko se iole ozbiljno bavi zavarivanjem.

Istovremeno odajem priznanje koleginicama, autorkama Metalurgije zavarivanja profesorkama Radici Prokić-Cvetković i Oliveri Popović, na načinu objašnjavanja metalurških pojava pri zavarivanju i sistematičnosti prikazivanja. Znajući koliki je napor uložen, da bi se ovakav materijal našao pred nama, najiskrenije čestitke.

Milica Antić, dipl.ing metalurg, EWE

P. Petrov [1,a], D. Kaisheva[1,b], G. Bokuchava[2,c], I. Papushkin[2,d], S. Valkov[1,e]

Investigation of Residual Stresses in Dissimilar Copper-Steel Joint Welded by Electron Beam

Ispitivanje zaostalih napona u raznorodnom spoju bakar-čelik zavarenom elektronskim snopom

Originalni naučni rad / Original scientific paper

Rad je u izvornom obliku objavljen u Zborniku sa 4. IIW Kongresa zavarivanja Jugoistočne Evrope „Safe Welded Construction by High Quality Welding" održanog u Beogradu 10-13. Oktobra 2018

Rad primljen / Paper received:
Oktobar 2019.

Adresa autora / Author's address:
[1] *Institute of Electronics, Bulgarian Academy of Sciences, 72 Tzarigradsko Chaussee, 1784 Sofia, Bulgaria*
[2] *Frank Laboratory of Neutron Physics, Joint Institute for Nuclear Research, 6 Joliot-Curie str., 141980 Dubna, Russia*
[a]*pitiv@ie.bas.bg,* [b]*darinakaisheva@abv.bg,* [c]*gizo@nf.jinr.ru,* [d]*piv@nf.jinr.ru,* [e]*stsvalkov@gmail.com*

Ključne reči: zavarivanje elektronskim snopom, raznorodni spojevi, neutronska difrakcija, zaostali naponi, mikrodeformacije

Key words: electron beam welding, dissimilar joints, neutron diffraction, residual stresses, microstrains

Abstract

The results of experimental determination of residual stress distribution in dissimilar materials welded by EBW method via neutron diffraction are presented. The joints between copper and stainless steel were investigated. Two samples with different beam current were welded. The residual stresses were measured using TOF diffraction method at a pulsed neutron source. The strain is determined by the relative change in the neutron time of flight. Analysis of the widths of the peaks made it possible to obtain information on microstrains in the samples. The residual stresses in copper do not exceed 100 MPa in both samples. The maximum stresses can be seen in the steel zone of thermal impact in the X component – 450 MPa.

Rezime

Prikazani su rezultati eksperimentalnog određivanja raspodele zaostalih napona u različitim materijalima zavarenim elektronskim snopom (EBW) pomoću difrakcije neutrona. Ispitivani su spojevi između bakra i nerđajućeg čelika. Zavarena su dva uzorka sa različitom strujom snopa. Zaostali naponi su mereni TOF metodom difrakcije na izvoru pulsirajućih neutrona. Deformacija se određuje relativnom promenom vremena proticanja neutron. Analiza širina vrhova omogućila je dobijanje informacija o mikrodeformacijama u uzorcima. Zaostali naponi u bakaru ne prelaze 100 MPa u oba uzorka. Maksimalni naponi se primećuju u zoni uticaja toplote čelika u X komponenti - 450 MPa.

1. Introduction

Electron beam welding is one of the modern methods of joining various refractory metals, dissimilar, chemically active, high-quality steels and high-strength alloys. The process of beam welding is characterized by two features: the welding process is realized in a vacuum environment, which guarantees obtaining the cleanest surface and degassing of the molten metal; heating occurs to very high temperatures, thus the metal melts quickly, and the seam results in a fine-grained and minimal width as a result of the treatment. Welding products composed of dissimilar materials makes it easier to join parts and improve the performance properties of structures based on them. Laser and electron beam welding greatly simplified the technology of welding of dissimilar materials.

1. Uvod

Zavarivanje elektronskim snopom je jedna od savremenih metoda spajanja različitih vatrootpornih metala, različitih, hemijski aktivnih, visokokvalitetnih čelika i legura visoke čvrstoće. Proces zavarivanja snopom karakterišu dve pojave: postupak zavarivanja se realizuje u vakuumu, što garantuje dobijanje najčistije površine i degazaciju rastopljenog metala; zagrevanje se dešava na veoma visokim temperaturama, pa se metal brzo topi, a šav rezultuje finim zrnom i minimalnom širinom. Zavarenim proizvodima sastavljenim od raznorodnih materijala olakšavaju spajanje delova i poboljšavaju karakteristike konstrukcija izrađenih od tih materijala. Lasersko i zavarivanje elektronskim snopom uveliko je pojednostavilo tehnologiju zavarivanja raznorodnih materijala.

After electron beam welding (EBW) residual stresses and strains are originated in welding joint and in heat affected zone (HAZ) [1, 2] as a result of differential contractions which occur as the weld metal solidifies and cools down to the ambient temperature. The residual stresses strongly affect on the structure and solidity of welding joint [3] and, consequently, on lifetime of the final product. Therefore it is necessary to control their level and spatial distribution after welding process.

Over many years, internal residual stresses in materials have been studied using various non-destructive techniques: X-ray diffraction, ultrasonic scanning, and various magnetic techniques (measurements of magnetic induction, permeability, anisotropy, Barkhausen effect, magnetoacoustic effects). However, all these methods have certain limitations. For example, using X-ray scattering and magnetic methods, only stresses near the material surface can be studied due to their small penetration depth; application of the magnetic methods is restricted to ferromagnetic materials. Moreover, the specimen texture has a significant effect on the results obtained by magnetic and ultrasonic methods. Among all these techniques, the neutron diffraction study of residual stresses has a special place, since, in contrast to conventional methods, neutrons can penetrate materials to a depth of 2–3 cm for steels and to 10 cm for aluminium. Other important advantages of the neutron diffraction technique include high spatial resolution, applicability for multiphase materials, non-destructive character of the method, possibility to characterize materials microstructure and defects (microstrain, coherently scattering crystallite size, dislocation density, etc.).

The main aim of the current research work was the experimental determination of residual stress distribution in the flat steel and copper plates welded by EBW method using high resolution neutron diffraction.

In this paper, we investigated the residual stresses in dissimilar joints between copper and stainless steel 304 welded by electron beam at different ~~welding speeds~~ beam current. Two identical samples (Fig.1) with size of 50x40x10 mm were welded in Institute of Electronics of Bulgarian Academy of Sciences (Sofia, Bulgaria) using Leybold Heraeus welding unit. Samples were prepared with a welding speed of 1 cm/s and U=55 kV. The first sample was prepared with a current I = 50 mA, second – I = 60 mA.

The neutron diffraction method was used to determine the residual stress distributions in both samples. The neutron experiments were performed

Nakon zavarivanja elektronskim snopom (EBW) nastaju zaostali naponi i deformacije u zavarenom spoju i u zoni uticaja toplote (HAZ-ZUT) [1,2] kao rezultat različitih skupljanja koje nastaju kada metal šava očvrsne i ohladi se do temperature okoline. Zaostali naponi značajno utiču na strukturu i čvrstoću zavarenog spoja [3], a samim tim i na životni vek krajnjeg proizvoda. Zbog toga je potrebno kontrolisati njihov nivo i prostornu raspodelu nakon zavarivanja.

Već više godina se proučavaju zaostali naponi u materijalima korišćenjem različitih tehnika bez razaranja: difrakcije rendgenskih zraka, ultrazvučnog skeniranja i različitih magnetnih tehnika (merenja magnetne indukcije, permeabilnosti, anizotropije, Barkhauzenovog efekta, magnetno-akustičkih efekata). Međutim, sve ove metode imaju određena ograničenja. Na primer, pomoću rasipanja rendgenskih zraka i magnetnih metoda, samo mali naponi u blizini površine materijala, se mogu proučavati zbog njihove male dubine prodiranja; primena magnetnih metoda ograničena je na feromagnetne materijale. Šta više, tekstura uzorka ima značajan uticaj na rezultate dobijene magnetnim i ultrazvučnim metodama. Među ovim tehnikama, kod ispitivanja zaostalih napona, difrakcija neutrona ima posebno mesto, jer za razliku od konvencionalnih metoda, neutroni mogu prodirati kroz materijale do dubine od 2 do 3 cm za čelik i do 10 cm za aluminijum. Ostale važne prednosti tehnike difrakcije neutrona su visoka prostorna rezolucija, primenljivost za višefazne materijale, nerazorni karakter metode, mogućnost karakterizacije mikrostrukture materijala i oštećenja (mikrodeformacije, koherentno rasipanje veličine kristalita, gustina dislokacija itd.).

Glavni cilj trenutnog istraživačkog rada bilo je eksperimentalno određivanje raspodele zaostalih napona u ravnim čeličnim i bakarnim limovima zavarenim EBW postupkom, pomoću difrakcije neutrona visoke rezolucije.

U ovom radu smo istražili zaostale napone u različitim spojevima između bakra i nerđajućeg čelika tipa 304, zavarenih elektronskim snopom, pri različitim jačinama snopa. Dva identična uzorka (slika 1) dimenzija 50x40x10 mm zavarena su u Institutu za elektroniku Bugarske akademije nauka (Sofija, Bugarska) pomoću Leibold Heraeus jedinice za zavarivanje. Uzorci su pripremljeni brzinom zavarivanja od 1 cm / s i U = 55 kV. Prvi uzorak je pripremljen sa strujom I = 50 mA, drugi - I = 60 mA.

Metoda difrakcije neutrona korišćena je za određivanje raspodele zaostalih napona u oba uzorka. Eksperimenti sa neutronima izvedeni su na

on the FSD diffractometer at the IBR-2 pulsed reactor in the Frank Laboratory of Neutron Physics, Joint Institute for Nuclear Research, Dubna, Russian Federation.

2. Method

Internal stresses existing in a material cause corresponding lattice strains, which, in turn, results in shifts of Bragg peaks in the diffraction spectrum. This yields direct information on changes in interplanar spacing in a gauge volume, which can be easily transformed into data on internal stresses, using known elastic constants of a material [4],

$$\frac{\left(d_{\exp}-d_0\right)}{d_0}=\frac{\Delta a}{a}\approx\frac{\sigma}{E} \quad (1)$$

where d_{exp} is the measured interplanar spacing, d_0 is the same interplanar spacing in a specimen without internal stresses, $\Delta a/a_0$ is the strain as the relative change in the unit cell parameter of a material, E is the Young's modulus of a material, and σ is the stress.

FSD difraktometru na impulsnom reaktoru IBR-2 u Frank laboratoriji za fiziku neutrona, Institut za nuklearna istraživanja, Dubna, Ruska Federacija.

2. Metoda

Unutrašnja naprezanja koja postoje u materijalu izazivaju odgovarajuće naprezanje rešetki, što zauzvrat dovodi do pomeranja Bragg-ovih vrhova u difrakcionom spektru. Ovo daje direktne informacije o promenama interplanarnog rastojanja u zapremini merača, koje se lako mogu transformisati u podatke o unutrašnjim naponima, koristeći poznate elastične konstante materijala [4],

$$\frac{\left(d_{\exp}-d_0\right)}{d_0}=\frac{\Delta a}{a}\approx\frac{\sigma}{E} \quad (1)$$

gde je d_{exp} izmereni interplanarni razmak, d_0 je isti međuplanarni razmak u uzorku bez unutrašnjih naprezanja, $\Delta a/a_0$ je naprezanje kao relativna promena parametra jedinične ćelije materijala, E je Jungov modul materijala, i σ je napon.

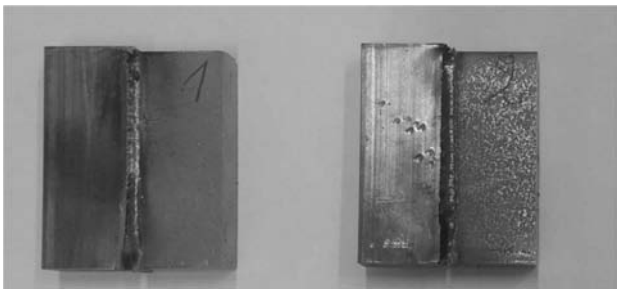

Sample1 *Sample2*

Figure 1. *Samples welded by electron beam welding. The left side is copper, right - steel.*
Slika 1. *Uzorci zavareni elektronskim snopom. Leva strana je bakar, desna - čelik.*

A scheme of the experimental design for determining internal stresses in a bulk object is presented in Fig. 1. Incident and scattered (at angles 2θ = ±90°) neutron beams are limited by diaphragms forming gauge volume in investigated specimen. Measurement of neutron diffraction spectra by ±90° detectors (Fig. 2) allows simultaneous determination of strains in two mutually perpendicular directions. The strain is measured in the direction parallel to the neutron scattering vector Q (Q1 and Q2). The specimen region under study is scanned using the gauge volume by moving the specimen in the required directions.

The incident beam is usually formed using cadmium or boron nitride diaphragms with characteristic sizes from 0.5–1 mm to several cm depending on the purpose of the experiment. To define a gauge volume of optimum shape in the studied specimen, at the scattered beam radial Soller collimators with many (about several tens) vertical slits formed by Mylar films with gadolinium

Šema eksperimentalnog koncepta za određivanje unutrašnjih napona u objektu prikazana je na Sl. 1. Upadajući i raspršeni (pod uglom 2θ = ± 90 °) snopovi neutron, ograničeni su dijafragmama koje formiraju merače zapremine u ispitivanom uzorku. Merenje spektra difrakcije neutrona pomoću detektora ± 90 ° (Sl. 2) omogućava istovremeno određivanje deformacija u dva međusobno normalna pravca. Napon se meri u pravcu paralelnom vektoru raspršivanja neutrona Q (Q1 i Q2). Područje uzorka koje se proučava, skenira se pomoću merača zapremine pomeranjem uzorka u traženim pravcima.

Upadni snop obično se formira pomoću dijafragmi od kadmijuma ili bora ili bor-nitrida, karakterističnih veličina od 0,5-1 mm do nekoliko cm, zavisno od svrhe eksperimenta. Da bi se definisala zapremina merača optimalnog oblika u ispitivanom uzorku, često se koristi rasuti snop uz radijalne kolimatore sa mnogo (oko nekoliko desetina) vertikalnih proreza oblikovanih Milar filmovima sa premazom gadolinijum oksida. Radijalni Soller kolimator

oxide coating are often used. A radial Soller collimator is placed at a sufficiently large (at least 150–250 mm) fixed distance from the specimen and provides high spatial resolution along the incident neutron beam direction (0.5–2 mm).

postavljen je na dovoljno velikoj (najmanje 150–250 mm) fiksnoj udaljenosti od uzorka i pruža veliku prostornu rezoluciju duž pravca upadajućeg neutronskog snopa (0,5–2 mm).

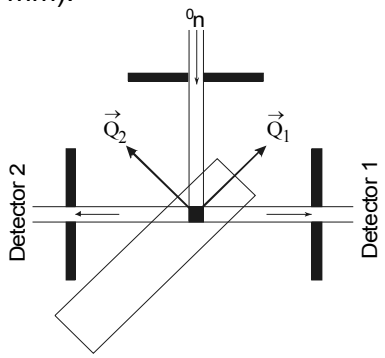

Figure 2. *Schematic of the experimental design for determining internal stresses in a bulk object. Incident and scattered (at angles 2θ = ±90°) neutron beams are restricted by diaphragms shaping a gauge volume within the specimen. Measurement of neutron diffraction patterns by ±90° detectors allows simultaneous determination of strains in two mutually perpendicular directions.*

Slika 2. *Šema eksperimentalnog koncepta za određivanje unutrašnjih napona u rasutom objektu. Upadni i raspršeni (pod uglom 2 θ = ± 90 °) neutronski zraci ograničeni su dijafragmama koje oblikuju merač zapremine unutar uzorka. Merenje uzoraka difrakcije neutrona detektorom od ± 90 ° omogućava istovremeno određivanje deformacijaa u dva međusobno normalna pravca.*

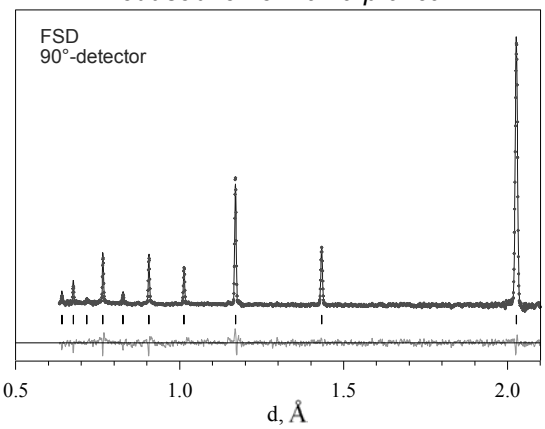

Figure 3. *Part of the diffraction spectrum of the α-Fe reference specimen, measured on the FSD neutron diffractometer in the high-resolution mode using 90°-detector. The experimental points, the profile curve calculated by the Rietveld method and difference curve are shown. Bars indicate diffraction peak positions.*

Slika 3. *Deo difrakcionog spektra referentnog uzorka α-Fe, mereno na FSD neutronskom difrakterometru u režimu visoke rezolucije, korišćenjem detektora 90 °. Prikazane su eksperimentalne tačke, kriva profila izračunata Rietveld-ovom metodom i kriva razlika. Trake označavaju pozicije vrha difrakcije*

The principle of the determination of the lattice strain is rather simple and it is based on the Bragg's law

$$2d_{hkl}\sin\theta = \lambda \qquad (2)$$

where λ is the neutron wavelength, dhkl is the interplanar spacing, and θ is the Bragg angle.

The neutron diffraction method is very similar to the X-ray technique. However, in contrast to the characteristic X-ray radiation the energy spectrum of thermal neutrons has a continuous character (Maxwellian distribution). The velocity of thermal neutrons is rather small and this gives the

Princip određivanja deformacije rešetke je prilično jednostavan i zasnovan je na Braggovom zakonu

$$2d_{hkl}\sin\theta = \lambda \qquad (2)$$

gde je λ talasna dužina neutrona, dhkl je interplanarni razmak, a θ je Bragg-ov ugao

Metoda difrakcije neutrona veoma je slična tehnici rendgenskih zraka. Međutim, za razliku od karakterističnog rendgenskog zračenja, energetski spektar toplotnih neutrona ima kontinuirani karakter (Makvellian distribucija). Brzina toplotnih neutrona je prilično mala i ovo daje priliku da se analizira

opportunity to analyse the neutron energy using it's time of flight during the experiment at a pulsed neutron source. When using TOF diffraction method at a pulsed neutron source, the strain is determined by the relative change in the neutron time of flight Δt/t. Depending on the neutron wavelength, the peak position on the time scale is defined by the condition [see 3]:

$$t = \frac{L}{v} = \frac{\lambda m L}{h} = \frac{2mLd_{hkl}\sin\theta}{h} \quad (3)$$

where L is the total flight distance from a neutron source to the detector, v is the neutron velocity, λ is the neutron wavelength, m is the neutron mass, h is Planck's constant, dhkl is the interplanar spacing, and θ is the Bragg angle.

Therefore, in case of TOF neutron diffraction the lattice strain is determined as

$$\varepsilon_{hkl} = \frac{\left(d_{hkl} - d^0_{hkl}\right)}{d^0_{hkl}} = \frac{\Delta t}{t} \quad (4)$$

where d_{hkl} and d^0_{hkl} are the interplanar spacing for strained and unstrained lattices, and *t* is the neutron time of flight.

An analysis of the shape (width in the simplest case) of diffraction peaks can yield information on lattice distortions in individual grains (microstrain) and their sizes [5]. This is especially convenient to do that using a TOF diffractometer with the functional dependence of the peak width on the interplanar spacing [7],

$$W^2 = C_1 + C_2 d^2 + C_3 d^2 + C_4 d^4 \quad (1)$$

where W is the peak width, C1 and C2 are the constants defining the diffractometer resolution function and known from measurements with a reference specimen, C3=(∆a/a)2 is the unit cell parameter dispersion (microstrain), and C4 is the constant related to the crystallite size.

3. Experiment

TOF neutron diffraction study of residual stresses in welded specimens was performed on FSD Fourier diffractometer [6, 7] at fast pulsed IBR-2 reactor in FLNP JINR, Dubna, Russia. FSD diffractometer is dedicated for residual stress studies in bulk industrial components and new advanced materials. A special correlation technique - a fast Fourier chopper for the primary neutron beam intensity modulation and the RTOF method for data acquisition - makes it possible to obtain high resolution neutron diffraction spectra Δd/d ≈ 2÷4×10-3.

During the experiment on the FSD neutron diffractometer a small scattering volume (gauge volume) of the size of 2x2x24 mm for EBW specimen were defined using radial collimators in front of the 90° detectors (Fig. 4). The specimens were scanned across weld regions along middle

energija neutron, koristeći vreme leta tokom eksperimenta na impulsnom izvoru neutrona. Kada se koristi difrakciona metoda TOF na izvoru impulsa neutrona, naprezanje se određuje relativnom promenom vremena leta neutrona Δt/t. Zavisno od talasne dužine neutrona, položaj vrha na vremenskoj skali je definisan uslovom (vidi 3]:

$$t = \frac{L}{v} = \frac{\lambda m L}{h} = \frac{2mLd_{hkl}\sin\theta}{h} \quad (3)$$

gde je L ukupna dužina leta od izvora neutrona do detektora, v je brzina neutrona, λ je talasna dužina neutrona, m je masa neutrona, h je Plankova konstanta, dhkl je interplanarni razmak, a θ je Bragg-ov ugao

Zbog toga se u slučaju TOF difrakcije neutrona, deformacija rešetke određuje kao

$$\varepsilon_{hkl} = \frac{\left(d_{hkl} - d^0_{hkl}\right)}{d^0_{hkl}} = \frac{\Delta t}{t} \quad (4)$$

gde su d_{hkl} i d^0_{hkl} interplanarni razmak za deformisane i nedeformisane rešetke, a *t* je vreme leta neutrona.

Analiza oblika (širina u najjednostavnijem slučaju) difrakcionih vrhova može dati informacije o izobličenjima rešetki u pojedinim zrnima (mikrodeformacija) i njihovim veličinama [5]. Ovo je posebno pogodno za korišćenje TOF-ovog difraktometra sa funkcionalnom zavisnošću širine vrha od interplanarnog razmaka [7],

$$W^2 = C_1 + C_2 d^2 + C_3 d^2 + C_4 d^4 \quad (2)$$

gde je W širina vrha, C1 i C2 su konstante koje definišu funkciju razlučivanja difraktometra i poznate su iz merenja sa referentnim uzorkom, C3=(∆a/a)2 je disperzija parametara jedinične ćelije (mikrodeformacija), a C4 je konstanta povezana sa veličinom kristalita

3. Eksperiment

Studija o zaostalim naponima TOF difrakcijom neutrona na zavarenim uzorcima izvedena je na FSD Fourier-ovom difraktometru [6, 7], na brzo pulzirajućem IBR-2 reaktoru u FLNP JINR, Dubna, Rusija. FSD difraktometar namenjen je studijama zaostalih naprezanja u različitim industrijskim komponentama i novim naprednim materijalima. Specijalna tehnika korelacije - brza Fourierov-a seckalica za modulaciju intenziteta primarnog snopa neutrona i RTOF metoda za prikupljanje podataka - omogućava dobijanje spektra difrakcije neutrona Δd/d ≈ 2÷4×10-3 visoke rezolucije.

Tokom eksperimenta na FSD neutronskom difraktometru, određeni su mali volumeni raspršivanja (zapreminska vrednost) veličine 2x2x24 mm za EBW uzorak pomoću radijalnih kolimatora ispred detektora od 90° (Sl. 4). Uzorci su skenirani na području šava duž srednje linije line of

the specimen thickness. Orienting a specimen in a certain way, the main components of residual strain in three mutual perpendicular directions (with respect to the direction of the neutron scattering vector Q) were measured.

debljine uzorka. Orijentišući uzorak na određeni način, merene su glavne komponente zaostalog naprezanja u tri međusobno normalna smera (u odnosu na smer vektora raspršivanja neutrona Q).

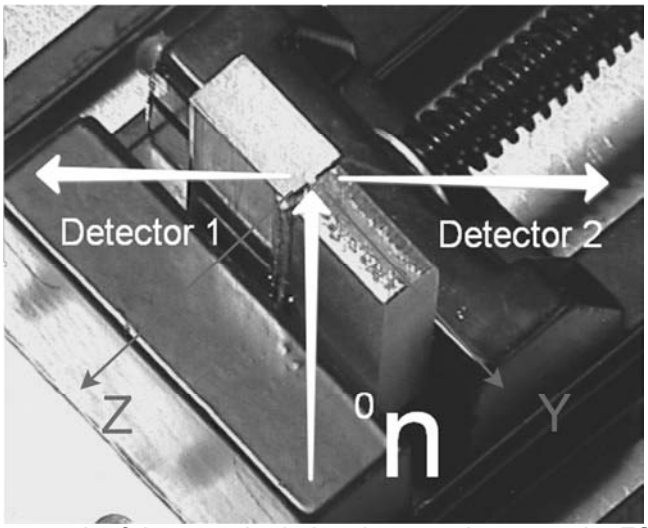

Figure 4. *Photograph of the sample during the experiment on the FSD instrument.*
Slika 4. *Fotografija uzorka tokom eksperimenta na FSD instrumentu.*

4. Results

Copper and steel have very different mechanical and physical properties. These features exerted a great influence on the stress distribution in the welded samples. The stress diagrams clearly show the difference between the two materials Fig. 5-6. The residual stresses in copper do not exceed 100 MPa in both samples. The maximum stresses can be seen in the steel zone of thermal impact in the X component. The first sample has lower stresses in the Z component than second sample. The residual stresses in the Y component in both cases are small, do not exceed 100 MPa.

4. Rezultati

Bakar i čelik imaju veoma različita mehanička i fizička svojstva. Ove karakteristike imale su veliki uticaj na raspodelu napona u zavarenim uzorcima. Dijagram naprezanja jasno pokazuje razliku između dva materijala. Sl. 5-6. Preostali naponi u bakru ne prelaze 100 MPa u oba uzorka. Maksimalni naponi se primećuju u zoni uticaja toplote na čeliku u X komponenti. Prvi uzorak ima niža naprezanja u komponenti Z u odnosu na drugi uzorak. Preostali naponi u Y komponenti u oba slučaja su mali, ne prelaze 100 MPa.

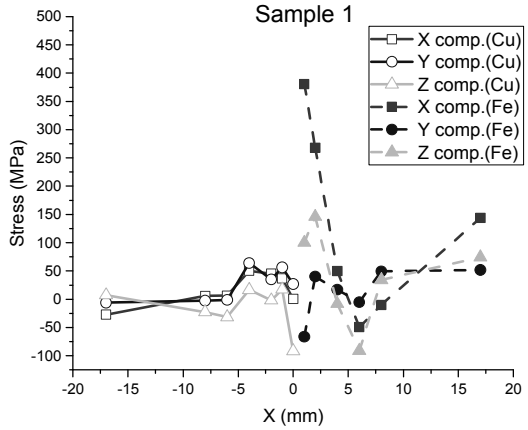

Figure 5. *Residual stress in the studied EBW specimen No. 1. (I = 50 mA)*
Slika 5. *Zaostlai naponi na proućavanom uzorku EWB Br. 1. (I = 50 mA)*

Analysis of the widths of the peaks made it possible to obtain information on microstrains in the samples (Fig. 7-8). The level of microstrains in the first sample is slightly higher than in the second. The discrepancy in the components far from welding indicates the presence of microstrains in the starting material.

Analiza širina vrhova omogućila je dobijanje podataka o mikrodeformacijama u uzorcima (slika 7-8). Nivo mikrodeformacija u prvom uzorku je neznatno viši nego u drugom. Nesklad u komponentama daleko od mesta zavarivanja ukazuje na prisustvo mikrodeformacija u početnom materijalu.

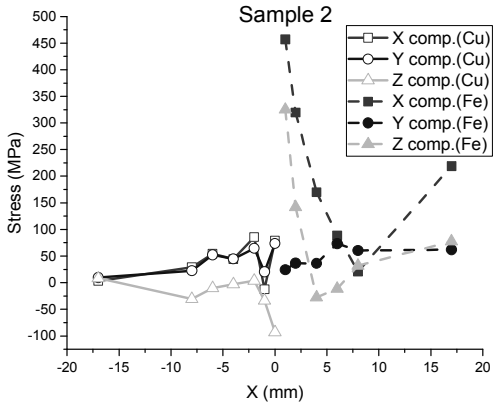

Figure 6. *Residual stress in the studied EBW specimen No. 2. (I = 60 mA)*
Slika 6. *Zaostlai naponi na proućavanom uzorku EWB Br. 2. (I = 60 mA*

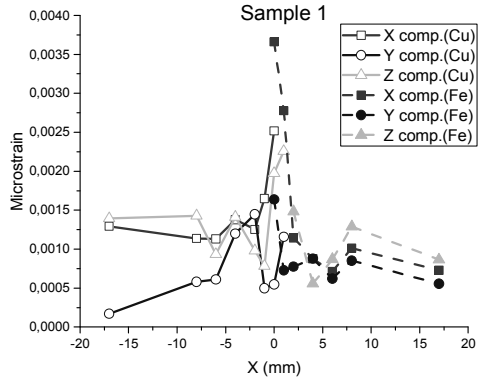

Figure 7. *Residual microstrain in the studied specimen No. 1. (I = 50 mA)*
Slika 7. *Zaostali naponi na proučavanom uzorku Br. 1. (I = 50 mA)*

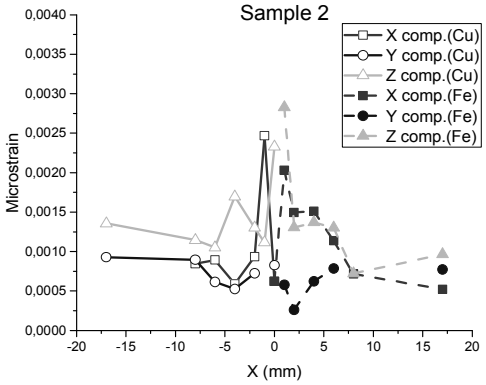

Figure 8. *Residual microstrain in the studied specimen No. 2. (I = 60 mA)*
Slika 8. *Zaostali naponi na proučavanom uzorku Br. 2. (I = 60 mA)*

Microstrains grow in the region of thermal influence in the X and Y component of copper and the X component of steel. Z components also vary in both materials, but less than in other components. Microstrains in the second sample differ significantly from the first. Z component practically does not change. The X component in the welding location has a dip almost to zero.

5. Conclusions

The residual stresses in dissimilar joints between copper and stainless steel 304 welded by electron beam at different beam current were investigated. Copper and steel have very different mechanical and physical properties. These features exerted a great influence on the stress distribution in the welded samples. The residual stresses in copper do not exceed 100 MPa in both samples. The maximum stresses can be seen in the steel zone of thermal impact in the X component – 450 MPa. The higher the beam current is, the higher the residual stresses are.

Acknowledgements

The work was partially supported by the Russian Foundation for Basic Research (project No. 15-08-06418_a) and the Bulgarian National Scientific Fund (Contract No. DN 07/26).

Mikrodeformacije rastu u području toplotnog uticaja u komponentama X i Y kod bakra i X komponenti kod čelika. Z komponente se takođe razlikuju u oba materijala, ali manje nego u ostalim komponentama. Mikrodeformacije u drugom uzorku značajno se razlikuju od prvog. Z komponenta se praktično ne menja. X komponenta na mestu zavarivanja ima pad skoro do nule.

5. Zaključci

Istraživani su zaostali naponi u različitim spojevima između bakra i nehrđajućeg čelika tipa 304 zavarenih elektronskim snopom pri različitim strujama snopa. Bakar i čelik imaju veoma različita mehanička i fizička svojstva. Ove karakteristike imale su veliki uticaj na raspodelu napona u zavarenim uzorcima. Preostali naponi u bakaru ne prelaze 100 MPa u oba uzorka. Maksimalni naponi se primećuju u zoni toplotnog uticaja kod čelika u X komponenti - 450 MPa. Što je veća struja snopa, veći su zaostali naponi.

Zahvalnost

Rad je delimično podržan od strane Ruske fondacije za osnovna istraživanja (projekat br. 15-08- 06418_a) i Bugarskog nacionalnog naučnog fonda (Ugovor br. DN 07/26).

References
Reference

[1] V. Michailov, V. Karkhin, P. Petrov “Principles of welding” Peter the Great St. Petersburg State Polytechnic University, 2016, 256p.
[2] Lindgren L.E., “Numerical modelling of welding”, Comput. Methods Appl. Mech. Eng., Vol. 195, Issue 48-49, pp. 6710-6736, 2006
[3] Turna M., Sahul M., Ondruska J and Lokaj J., “Electron beam welding of copper to stainless steel” Annals of DAAAM for 2011 & Proceedings of the 22nd International DAAAM Symposium, Volume 22, No.1
[4] Allen A.J., Hutchings M.T., Windsor C.G., “Neutron diffraction methods for the study of residual stress fields”, Advances in Physics, Vol. 34, No. 4, pp. 445-473, 1985
[5] Mittemeijer E.J., Welzel U., “The 'state of the art' of the diffraction analysis of crystallite size and lattice strain”, Z. Kristallogr., Vol. 223, pp. 552-560, 2008
[6] Bokuchava G.D., Aksenov V.L., Balagurov A.M. et al. “Neutron Fourier diffractometer FSD for internal stress analysis: first results”, Applied Physics A: Materials Science & Processing, Vol.74 [Suppl1], pp. 86-88, 2002
[7] Bokuchava G.D., Balagurov A.M., Sumin V.V., Papushkin I.V., “Neutron Fourier diffractometer FSD for residual stress studies in materials and industrial components”, Journal of Surface Investigation. X-ray, Synchrotron and Neutron Techniques, Vol. 4, No. 6, pp. 879-890, 2010

S. Medvedev[1,a], K. Klimau[1,b]

Computer and supercomputer technologies constructive-technological designing of responsible welded constructions
Kompjuterske i superkompjuterske tehnologije konstruktivno-tehnološkog projektovanja odgovornih zavarenih konstrukcija

Originalni naučni rad / Original scientific paper
Rad je u izvornom obliku objavljen u Zborniku sa 4. IIW Kongresa zavarivanja Jugoistočne Evrope „Safe Welded Construction by High Quality Welding" održanog u Beogradu 10-13. Oktobra 2018

Rad primljen / Paper received:
Oktobar 2019.
Ključne reči: zavarena konstrukcija; konstruktivno-tehnološko projektovanje; stanja napon-deformacija; superračunari

Adresa autora / Author's address:
[1] *United Institute of Informatics Problems of the National Academy of Sciences of Belarus, Surganov str. 6, 220012, Minsk, Belarus*
[a]*medv@newman.bas-net.by,* [b]*rembrand80@mail.ru*

Key words: welded construction; constructive-technological designing; stress-strain states; supercomputers

Abstract
Modern idea of the design and technological design of welded structures using the latest digitalization and classical approaches. Visionary generalization of ideas for scientific and technological breakthrough in the assembly and welding process.

Welding and related technologies that make a significant contribution to the creation of gross national products of developed countries cannot remain aloof from the processes of digitalization of economies and the construction of a new postindustrial society. At the same time, intellectual procedures for the development, modeling and finalization of the design of basic welded structures operating under variable loads, are crucial. It determines the carrying capacity and resource of the technical facilities and systems being developed, as well as the structure, equipment and organization of assembly and welding operations, especially in serial manufacturing. Multivariate development of welded structures has a clearly expressed constructive and technological character. This provision was first substantiated in the works of Professor N.O. Okerblom [1]. Since the middle of the last century, this position was cautious, but later the principles of constructive and technological design of welded structures received scientific recognition, also in the International Institute of Welding. Simultaneous (parallel) design of welded structures and development of welding technologies on the basis of calculation methods was supplemented in work with scientific and methodological approaches and with the corresponding software complex for automated design of technologically necessary assembly and welding fixtures [2]. Three-dimensional solid-state computer model of a welded structure and welds

Rezime
Savremena ideja projektovanja i tehnološkog projektovasnja zavarenih konstrukcija koja koristi najnoviju digitalizaciju i klasične pristupe. Vizionarsko uopštavanje ideja za naučni i tehnološki proboj u postupku montaže i zavarivanja.
Zavarivanje i srodne tehnologije koje daju značajan doprinos stvaranju bruto nacionalnih proizvoda razvijenih zemalja ne mogu ostati podalje od procesa digitalizacije ekonomija i izgradnje novog postindustrijskog društva. Istovremeno, ključni su intelektualni postupci za razvoj, modeliranje i finalizaciju projektovanja osnovnih zavarenih konstrukcija koje rade pod različitim opterećenjima. Određuje nosivost i resurse tehničkih sredstava i sistema koji se razvijaju, kao i strukturu, opremu i organizaciju montaže i zavarivanja, posebno u serijskoj proizvodnji.
Multivarijantni razvoj zavarenih konstrukcija ima jasno izražen konstruktivan i tehnološki karakter. Ova odredba prvi put je potvrđena u radovima profesora N.O. Okerblom [1]. Od sredine prošlog veka ova pozicija je bila oprezna, ali kasnije su principi konstruktivnog i tehnološkog projektovanja zavarenih konstrukcija dobili naučno priznanje, takođe i u Međunarodnom institutu za zavarivanje.
Istovremeno (paralelno) projektovanje zavarenih konstrukcija i razvoj tehnologija zavarivanja na osnovu metoda proračuna dopunjen je u radu, naučnim i metodološkim pristupima i odgovarajućim softverskim kompleksom za automatizovano projektovanje tehnološki neophodnih montažnih i zavarivačkih instalacija [2]. Trodimenzionalni računarski model stanja čvrstoće zavarene konstrukcije i zavarenih proizvoda postaje glavni izvor i nosilac projektnih i tehnoloških informacija.

becomes the main source and carrier of design and technological information.

The principles of design proposed by N.O. Okerblom, supplemented by the approach to the parallel design of technological tooling, found methodological confirmation in the concept of integrated information systems supporting all stages of the life cycle of technical objects and systems (so-called CALS-technology). It speaks of the correctness of direction of research and applied research conducted by the authors.

It is not possible to provide the process of constructive and technological development of welded structures, made of ordinary quality steels and low-alloy steels by arc welding methods, without in-depth analysis of possible internal residual stresses and deformations. Large numbers of scientific works were devoted to this direction both at the early stage of development of welding technology and at the present time. In the era of active computerization of the processes of engineering objects designing, commercial systems for finite element analysis like Ansys, Nastran, Marc, etc. are widely used for these purposes. Special software products (SYSWELD) are created by leading companies (for example, ESI Group) to simulate virtually all thermodynamic processes at welding and hardening. However, in commercial products, the features of welding technologies have not yet been adequately reflected, and specialized software products such as SYSWELD, Simufact Welding (MSC-software) are often too expansive for enterprises.

The approaches of computer forecasting of the stress-strain state (SSS) of welded constructions on the basis of the analysis of well-known works and simplified theories of occurrence of residual stresses and deformations are proposed in [4, 5]. At the initial stages of research, development of Vinokurov's approaches [3] seemed expedient on fictitious shrinkage longitudinal and transverse forces. However, further research and computational supercomputer experiments by commercial LS-DYNA system of nonlinear finite element analysis have refuted to some extent the existence of a fictitious shrink force and confirmed the expressed by N.O. Okerbolom in the 40s of the last century the idea of a mobile three-dimensional area of the weld, which is in a complex three-dimensional stress state.

The study of other authors, as well as instrumental measurements on real welded samples and welded structures, showed that mentioned above stresses are very close to the yield point of the base metal [7]. The ideas of the authors of [4,5], found

Principi projektovanja koje je predložio N.O. Okerblom, dopunjen pristupom paralelnog projektovanja tehnološkog alata, pronašao je metodološku potvrdu u konceptu integrisanih informacionih sistema koji podržavaju sve faze životnog ciklusa tehničkih objekata i sistema (tzv. CALS-tehnologija). Govori o ispravnosti smera i primenjenih istraživanja od strane autora.

Nije moguće obezbediti proces konstruktivnog i tehnološkog razvoja zavarenih konstrukcija, izrađenih od čelika običnog kvaliteta i niskolegiranih čelika postupcima elektrolučnog zavarivanja, bez dubinske analize mogućih unutrašnjih zaostalih naprezanja i deformacija. Ovom pravcu posvećen je veliki broj naučnih radova, kako u ranoj fazi razvoja tehnologije zavarivanja, tako i u današnje vreme. U doba aktivne informatizacije procesa projektovanja inženjerskih objekata, u te svrhe se široko koriste komercijalni sistemi za analizu konačnih elemenata poput Ansis, Nastran, Marc, itd. Posebne softverske proizvode (SISVELD) kreiraju vodeće kompanije (na primer, ESI Group) kako bi simulirale gotovo sve termodinamičke procese zavarivanja i otvrdnjavanja. Međutim, u komercijalnim proizvodima, karakteristike tehnologija zavarivanja još uvek nisu adekvatno odražene, a specijalizovani softverski proizvodi poput SISVELD, Simufact Velding (MSC-softver) su često previše skupi za preduzeća.

Pristupi računarskog predviđanja stanja naprezanja (SSS) zavarenih konstrukcija na osnovu analize dobro poznatih radova i pojednostavljenih teorija pojave zaostalih napona i deformacija predloženi su u [4, 5]. U početnim fazama istraživanja, Vinokurov pristup [3] činio se svrsishodnim na fiktivnom smanjivanju uzdužnih i poprečnih sila. Međutim, dalja istraživanja i računarski eksperimenti superkompjutera komercijalnim LS-DYNA sistemom nelinearnih analiza konačnih elemenata u određenoj su meri opovrgli postojanje fiktivne sile skupljanja i potvrdili iskaz N.O. Okerbolom koji je 40-ih godina prošlog veka zamenio mobilnu trodimenzionalnu oblast zavarenog spoja, koja je u složenom trodimenzionalnom naponskom stanju.

Studija drugih autora, kao i instrumentalna merenja stvarnih zavarenih uzoraka i zavarenih konstrukcija, pokazali su da su pomenuti naponi vrlo blizu naponu tečenja osnovnog materijala [7]. Ideje autora [4,5] našle su teorijsku i praktičnu potvrdu u radu japanskih kolega [6]. Savremena sredstva za geometrijsko modeliranje i izradu stanja čvrstoće pomoću 3D modela zavarenih konstrukcija kao što su SolidVorks, Inventor, NKS, ProE, itd., Kao i ugrađeni (ili se zasebno koriste) univerzalni

theoretical and practical confirmation in the work of Japanese colleagues [6]. Modern means of geometric modeling and construction of solid-state 3D models of welded structures and welds such as SolidWorks, Inventor, NX, ProE, etc., as well as built-in (or used separately) universal program modules of classical finite element analysis, linked to original approaches authors for computer forecasting of SSS, allow to present the scheme for integrating the processes of design of welded structures (Fig. 1). The bi-directional arrows in Fig. 1 emphasize the parallel (simultaneous) nature of all design and engineering procedures. Operational reflection of the interaction of the internal SSS of the welded structure with external loads allows more reasonably to see the influence of technological heredity on the behavior of the structures in real operation.

programski moduli klasične analize konačnih elemenata, povezani sa originalnim pristupima autora za računarsko predviđanje SSS-a, omogućavaju da predstave šemu za integrisanje procesa projektovanja zavarenih konstrukcija (slika 1). Dvosmerne strelice na slici 1 naglašavaju paralelnu (istovremeno) prirodu svih procedura projektovanja i inženjeringa. Operativni odraz interakcije unutrašnjih SSS zavarene konstrukcije sa spoljnim opterećenjima omogućava razumnije sagledavanje uticaja tehnološkog okruženja na ponašanje konstrukcija u stvarnom radu.

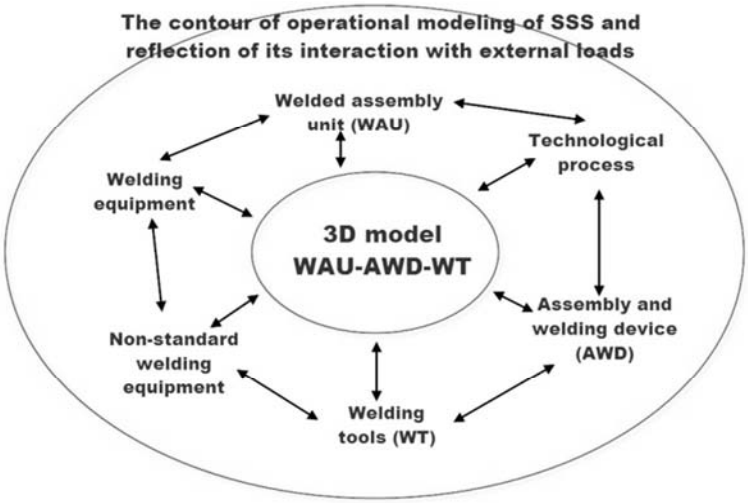

Figure 1. *Scheme of integrating the processes of design and technological design of welded structures of general purpose*

Slika 1. *Shema integrisanja procesa projektovanja i tehnološkog projektovanja zavarenih konstrukcija opšte namene*

Proposed scheme provides the ability to track the change in the resulting SSS welded structure, taking into account the design of the rigging, installation and clamping schemes, assessing the availability (reachability) of welded seams by welding tools, given the orientation of the tools, taking into account the results of a computer or automated work in the system of welding engineer fixture design instrument (INSVAR).

On modern welded structures operating under difficult operating conditions under dynamic loads, the total length of auxiliary and main welds can reach tens and hundreds of meters.

So as an example the length of welds on the supporting frame of a 220 tons mining truck exceeds several kilometers. To analyze the SSS of such responsible welded structures, especially under conditions of dynamic loading, traditional personal computer equipment and even graphic

Predložena šema pruža mogućnost praćenja promene rezultirajuće SSS zavarene konstrukcije, uzimajući u obzir projektovanje ugradnje, instalacije i stezanja, procenjujući dostupnost (dostižnost) zavarenih šavova zavarivačkim alatima, vezano za orijentaciju alata, uzimajući u obzir rezultate računarskog ili automatizovanog rada u sistemu instrumenata za projektovanje inženjera zavarivanja (INSVAR).

Na modernim zavarenim konstrukcijama koje rade pod otežanim uslovima rada pod dinamičkim opterećenjima, ukupna dužina pomoćnih i glavnih zavarenih spojeva može dostići desetine i stotine metara.

Kao primer, dužina zavara na nosećem ramu rudarskog kamiona od 220 tona prelazi nekoliko kilometara. Za analizu SSS tako odgovornih zavarenih konstrukcija, posebno u uslovima dinamičkog opterećenja, tradicionalna oprema za

stations is clearly not sufficient. To simulate similar processes and phenomena the authors have successfully used the capabilities of the national scientific and educational Grid-network of the Republic of Belarus with high-performance supercomputers of SKIF family (www.uiip.bas-net.by). The designers of engineering constructions can get remote access to these resources with the developed licensed software through the Internet from computers located at their workplaces.

Figure 2 shows a scheme for comprehensive compression of the zone of irreversible plastic deformations, whose outer boundary is generally limited to an isotherm at 600 ° C. Attention is drawn to the fact that the cross section of the seam (as the theory of welding stresses and deformations says) is stretched in the cross section.

lični računar, pa čak i grafičke stanice, očito nije dovoljna. Da bi simulirali slične procese i pojave, autori su uspešno koristili mogućnosti nacionalne naučne i obrazovne Grid mreže Republike Belorusije sa visoko performansnim superračunarima porodice SKIF (vvv.uiip.bas-net.bi). Projektanti inženjerskih konstrukcija mogu dobiti udaljeni pristup tim resursima pomoću razvijenog licenciranog softvera putem Interneta sa računara koji se nalaze na njihovim radnim mestima.

Na slici 2 prikazana je šema za sveobuhvatno sabijanje zone nepovratnih plastičnih deformacija, čija je spoljna granica uglavnom ograničena na izotermu na 600°C. Pažnja se skreće na činjenicu da je poprečni presek šava (kako teorija zavarivanja naglašava a deformacije kažu) je rastegnut po preseku.

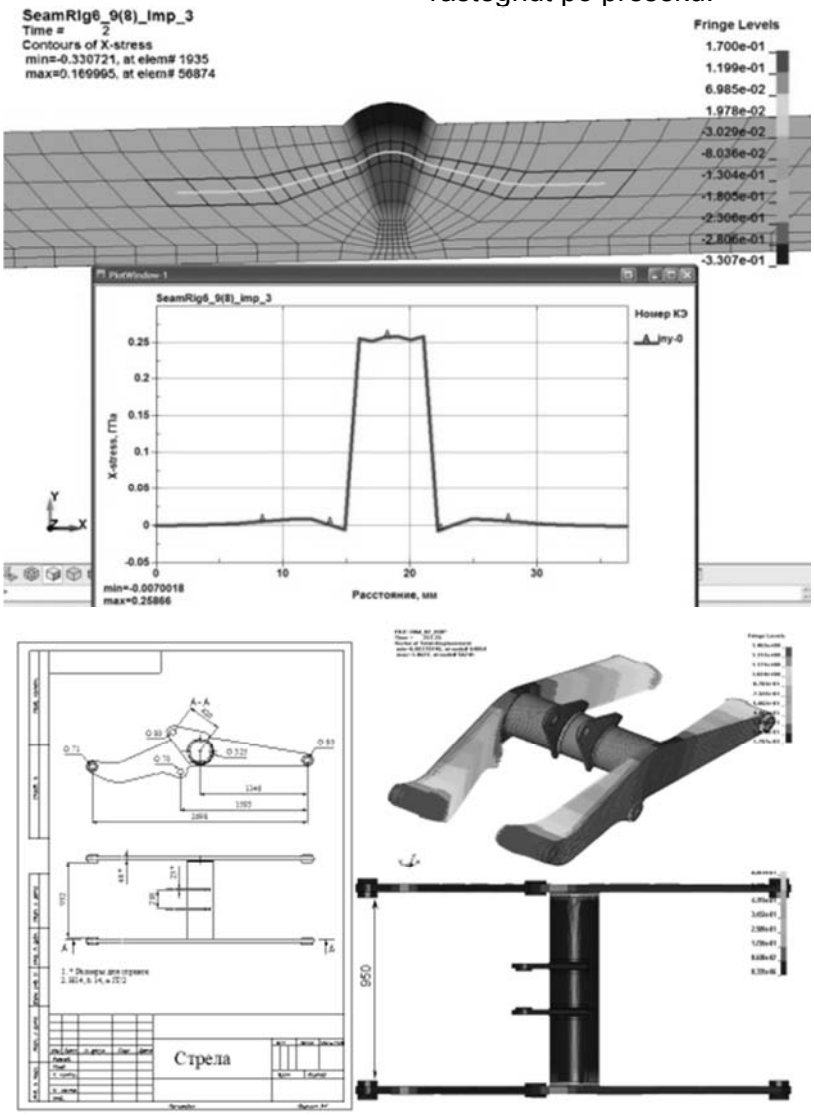

Figure 2. *Comprehensively compressed weld zone and an example of the prediction of total residual welding deformations*

Slika 2. *Sveobuhvatno sabijena zona zavarivanja i primer predviđanja ukupnih zaostalih deformacija usled zavarivanja*

Several assembly and welding fixtures designed in INSVAR are shown in Figure 3. The designer engineer of the tooling first determines the most rational position of the welding structure in 3D space during assembly and welding, then he fixes his technological design in special environment in the form of a schematic diagram of the device, then he indicates the preferred types and design parameters of the installation elements, fixation and clamps. Further, the software complex, according to its original algorithms, places the functional elements in relation to three-dimensional model of the welded structure and then unites them with the selected type of housing and later generates automatically the assembly drawing of the device structure on several projections on the projection connection. The specification of the assembly drawing is automatically generated, as well as the assembly drawings of the original parts and the selected housing type. On the housing drawing all the holes for installation on the body of functional elements are coordinated.

Na slici 3. prikazano je nekoliko montažnih i zavarivačkih elemenata dizajniranih u INSVAR-u. Inženjerski projektant alata prvo utvrđuje najracionalniji položaj zavarivačke konstrukcije u 3D prostoru tokom montaže i zavarivanja, a zatim svoj tehnološki projekat fiksira u posebnom okruženju u obliku šematskog dijagrama uređaja, onda on ukazuje na poželjne tipove i konstrukcijske parametre instalacionih elemenata, fiksatora i stezaljki. Nadalje, softverski kompleks, prema svojim originalnim algoritmima, postavlja funkcionalne elemente u odnosu na trodimenzionalni model zavarene konstrukcije, a zatim ih ujedinjuje s odabranim tipom kućišta, a kasnije automatski generiše sklopni crtež strukture uređaja na nekoliko projekcije na projekcijskoj vezi. Specifikacija crteža za montažu automatski se generiše, kao i sklopni crteži originalnih delova i odabranog tipa kućišta. Na crtežu na kućištu su koordinate svih otvora za ugradnju na telo funkcionalnih elemenata.

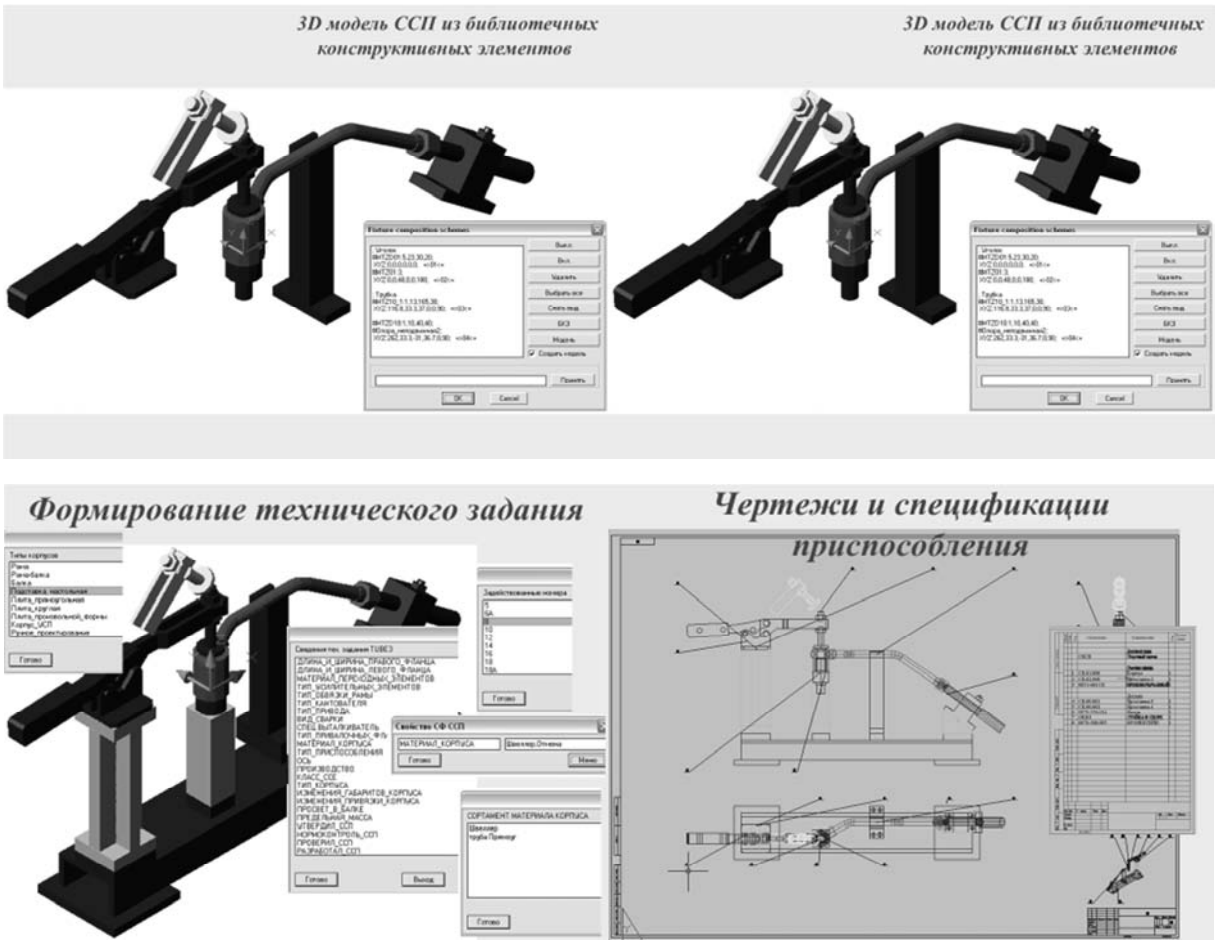

Figure 3. *An example of the design of an assembly and welding device formed by the INSVAR software packag*
Slika 3. *Primer dizajna uređaja za montažu i zavarivanje formiranog softverskim paketom INSVARe*

On the Figure 4 as an example pre-stressed after welding structure of the skeleton of an armored vehicle is subjected to a virtual impact of a shock blast wave. The displacements and stresses after explosion on the same structural elements are different, and this difference can be even more pronounced in the case of repeated short-term loads and prolonged operation.

Na slici 4, je dat primer prednapregnute nakon zavarivanja, konstrukcije skeleta oklopnog vozila koja je izložena je virtuelnom uticaju udarnog talasa. Pomeranja i naprezanja nakon eksplozije na istim konstrukcijskim elementima su različita, a ta razlika može biti još izraženija u slučaju ponovljenih kratkotrajnih opterećenja i produženog rada.

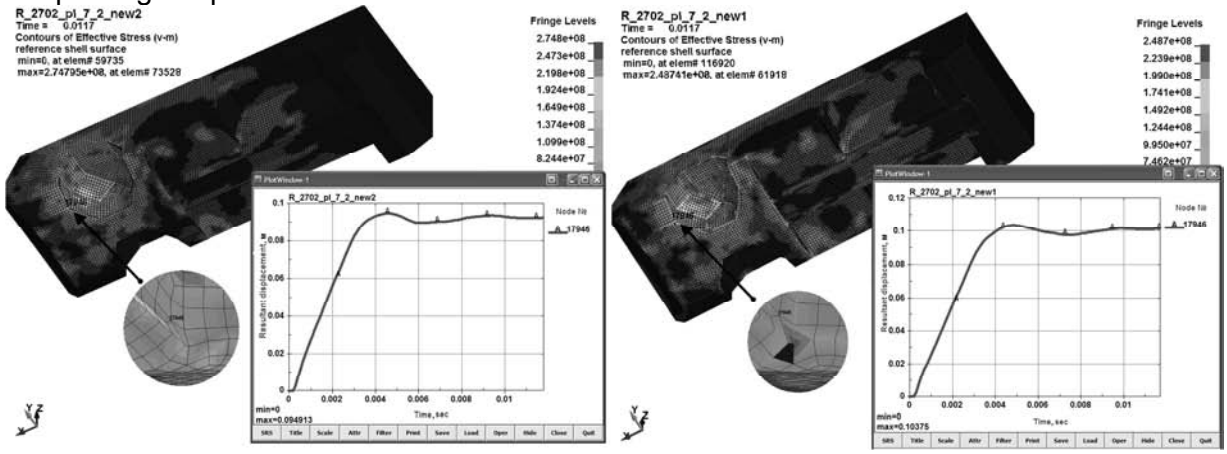

Figure 4 *Difference in movements of isotropic and welded structuresat the same dynamic impact*
Slika 4 *Razlika u kretanju izotropnih i zavarenih konstrukcija pod istim dinamičkim uticajem*

Figure 5 again confirms the well-known welding position that welded joints made without obvious defects under dynamic loads are destroyed in heat-affected zone or on the main material.

Slika 5 ponovo potvrđuje dobro poznati položaj zavarivanja tako da se izvedeni zavareni spojevi bez očiglednih oštećenja pod dinamičkim opterećenjima uništavaju u zoni uticaja toplote ili osnovnog materijalu.

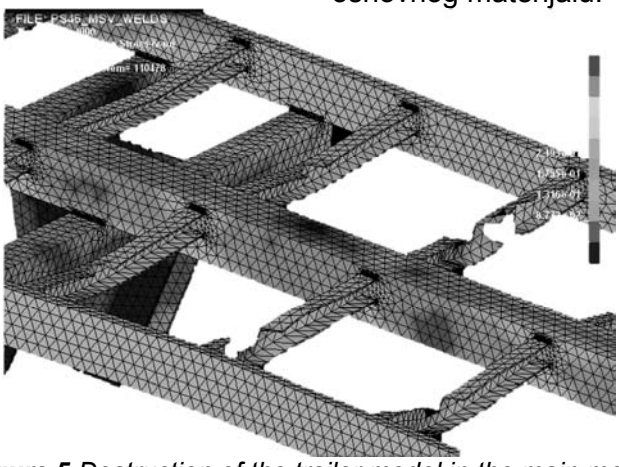

Figure 5 *Destruction of the trailer model in the main metal*
Slika 5 *Uništavanje modela prikolice u osnovnom materijalu*

Computer and supercomputer technologies for the design and technological design of welded structures are used by a number of Belarusian enterprises with a developed assembly and welding process. With their help, students are trained at the Department of Powder Metallurgy, Welding and Technology of Materials of the Belarusian National Technical University by carrying out course and diploma theses. The engineering and technical personnel of new formation, mastering the methods of constructive and technological design of welded structures using supercomputer, grid and cloud technologies, are able to provide a certain scientific and technological breakthrough in the assembly and welding process (Figure 6). The authors try to take the attention of scientists, designers, engineers and university teachers to this kind of mutually beneficial work.

Računarske i superračunarske tehnologije za projektovanje i tehnološko projektovanje zavarenih konstrukcija koriste mnoga beloruska preduzeća sa razvijenim postupkom montaže i zavarivanja. Uz njihovu pomoć, studenti se obučavaju na Katedri za metalurgiju praha, zavarivanje i tehnologiju materijala Beloruskog nacionalnog tehničkog univerziteta izvođenjem kurseva i izradom diplomskih radova. Inženjerski i tehnički kadar nove formacije, koji savladavaju metode konstruktivnog i tehnološkog rojektovanja zavarenih konstrukcija korišćenjem superračunarske, mrežne i tehnologije oblaka, u stanju su da pruže izvestan naučno-tehnološki iskorak u postupku montaže i zavarivanja (slika 6). Autori pokušavaju da skrenu pažnju naučnika, projektanata, inženjera i univerzitetskih nastavnika na ovakav obostrano koristan rad.

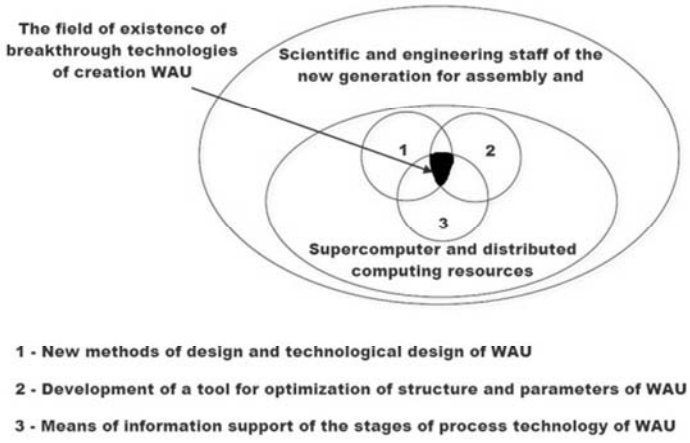

Figure 6 *Scheme of the appearance of the area of scientific and technological breakthrough in the development of promising welded structures*
Slika 6. *Šema pojave područja naučnog i tehnološkog proboja u razvoju perspektivnih zavarenih konstrukcija*

Conclusion

1. The authors have promoted the principles of constructive and technological design of welded structures, recognized by the world welding community, formulated by N.O. Okerblom, on infrastructural and computational level.
2. Approaches N.O. Okerblom is supplemented by a powerful functional and software tools for automated design of the assembly and welding fixtures, stands, conductors, etc.
3. Original methods and computer software, based on simplified theories of welding stresses and deformations, allow to predict the nature and magnitude of residual welding deformations with sufficient for engineering practice accuracy, also including taking into account the effect of fastening in technological equipment.

Zaključak

1. Autori su promovisali principe konstruktivnog i tehnološkog projektovanja zavarenih konstrukcija, priznata od strane svetske zajednice za zavarivanje, koje je formulisao N.O. Okerblom, na infrastrukturnom i računarskom nivou.
2. Pristup N.O. Okerblom-a je dopunjen snažnim funkcionalnim i softverskim alatima za automatizovano projektovanje montažnih i zavarivačkih instalacija, postolja, provodnika itd.
3. Originalne metode i računarski softver, zasnovan na pojednostavljenim teorijama napona i deformacija usled zavarivanja, omogućavaju predviđanje prirode i veličine zaostalih deformacija usled zavarivanja dovoljnim za tačnost inženjerske prakse, uključujući i efekat pričvršćivanja na tehnološkoj opremi.

References
Literatura

[1] Okerblom N.O. Structural and technological design of welded structures. –M. – L.: Mechanical engineering, 1964. – p. 420.
[2] Medvedev S.V. Computer modeling of residual welding strains in technological design of welded structures // Welding International. – 2002. – vol.16(1). – P.59-65.
[3] P. Zeng, Y. Gao, L. P. Lei. Welding process simulation under varying temperatures and constraints // Materials Science and Engineering: A, Volume 499, Issues 1–2, 15 January 2009, Pages 287-292.
[4] Klimau K., Medvedev S. Prognosis supercomputer modeling of welded structures behavior under dynamics loads // The 20th Scientific Slovak-Polish conference «Machine modeling and simulations 2015» September 7 - 9, Terchov, Slovak Republic, Trencin Alexander Dubcek University; Puchov: Faculty of Industrial technologies, 2015. – P.21 – 27.
[5] Medvedev S.V. Computer technologies of design of assembly and welding equipment – Minsk: Institute of Technical Cybernetics NAN Belarus, 2000. – 194 p.
[6] Vinokurov V.A. Theory of welding deformations and stresses. -M .: Mechanical engineering, 1984. – 280 p.
[7] 4. Medvedev S.V. Computer simulation of residual deformations in technological design of welded structures // Welding. - 2001. - № 8. - P.10-18.
[8] Medvedev S.V, Klimov K.A. Forecast supercomputer modeling of the behavior of welded structures under dynamic loads // Izvestiya TulGU. Technical science. Issue. 6 in 2 parts. Tula: Publishing House of Tula State University, 2015. - P.201 - 210.

P. Tashev[1a], H. Kondov[1b], E. Tasheva[2c]

Improvement of the properties of layers obtained by surfacing using TiN and SiC nanoparticles

Poboljšanje svojstava slojeva dobijenih navarivanjem pomoću nanočestica TiN i SiC

Originalni naučni rad / Original scientific paper

Rad je u izvornom obliku objavljen u Zborniku sa 4. IIW Kongresa zavarivanja Jugoistočne Evrope „Safe Welded Construction by High Quality Welding" održanog u Beogradu 10-13. Oktobra 2018

Rad primljen / Paper received:
Oktobar 2019.

Adresa autora / Author's address:
1 Institute of Metal Science, Equipment and Technologies with Hydroaerodynamics Centre "Acad. A. Balevski" – Bulgarian Academy of Sciences, 67 Shipchenski prohod, 1574 Sofia, Bulgaria
2 158, Todor Kableshkov Higher School of Transport, Geo Milev Str., 1574 Sofia, Bulgaria
E-mail: a ptashev@ims.bas.bg , b hriko61@gmail.com , c elitasheva@abv.bg

Ključne reči: Navarivanje nanočestice, obložene elektrode, tvrdoća, otpornost na habanje

Key words: Surfacing, nanoparticles, coated electrodes, hardness, wear resistance

Abstract

In the paper, investigation results are presented, the objective was to improve the mechanical characteristics (hardness and wear resistance) of layers produced by surfacing using TiN and SiC nanoparticles in coated electrodes (SMAW process). The two parameters were controlled by varying the introduced nanoparticles. Metallographic investigation of selected samples have been carried out and the microstructure changes have been established.

Introduction

The development of technics and technologies outlines new horizons for improvement of the welding technology and the materials used are refined. There is a tendency to increase the performance of overlay metal by using innovative coated electrodes for process 111 with introduced nanoparticles [1 - 4]. Studies on the effect of nanoparticles of various refractory compounds introduced in the coating of the welding electrodes show good tendencies in terms of increase in hardness and wear resistance [5, 6].

Experiments

Developed is a series of electrodes for SMAW based on electrodes grade E300, which contain TiN and SiC nano particles with dimensions about 50 nm in concentrations 0.1, 0.2, and 0.8 weight percent. For better absorption of the nano particles, "activation" in planetary mill with iron powder is carried out in advance. The particles are introduced during the preparation of the mixture for coating on the step of wet homogenization. The coating is pressed and dried according to the traditional manufacture recipe Fig. 1 [7].

Rezime

U radu su predstavljeni rezultati ispitivanja, čiji je cilj bio da se poboljšaju mehaničke karakteristike (tvrdoća i otpornost na habanje) slojeva dobijenih navarivanjem pomoću TiN i SiC nanočestica u obloženim elektrodama (SMAW-REL postupak). Dva parametra su kontrolisana variranjem uvedenih nanočestica. Obavljeno je metalografsko istraživanje odabranih uzoraka i utvrđene su promene mikrostrukture

Uvod

Razvoj tehnike i tehnologija ocrtava nove horizonte za poboljšanje tehnologije zavarivanja i korišćenih materijala. Postoji tendencija povećanja performansi metala koji se nanosi orišćenjem inovativnih obloženih elektroda za postupak 111 sa uvedenim nanočesticama [1 - 4]. Studije o uticaju nanočestica različitih vatrostalnih jedinjenja uvedenih u obloge elektroda pokazuju dobre tendencije u pogledu povećanja tvrdoće i otpornosti na habanje [5, 6].

Eksperimenti

Razvijen je niz elektroda za SMAW zasnovanih na elektrodama klase E300, koje sadrže nanočestice TiN i SiC dimenzija oko 50 nm u koncentracijama 0,1, 0,2 i 0,8 masenih procenata. Za bolju apsorpciju nanočestica, „aktiviranje" u planetarnom mlinu železnim prahom vrši se unapred. Čestice se unose tokom pripreme smeše za oblaganje na koraku vlažne homogenizacije. Obloga se presuje suši u skladu s tradicionalnom proizvodnom recepturom Sl. 1 [7].

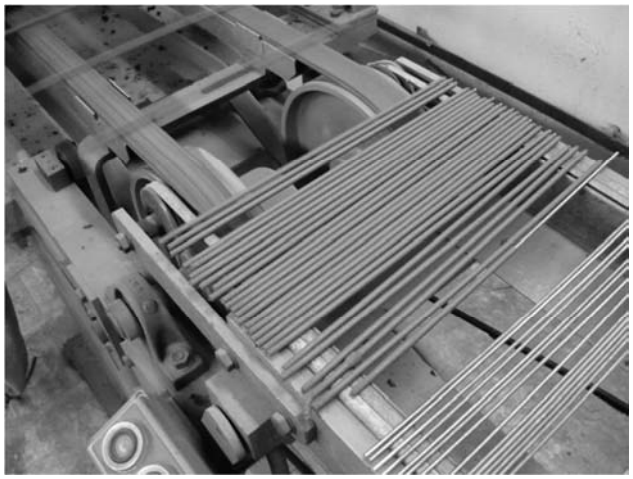

Figure 1. *Manufacture line for pressing of the coating*
Slika 1. *Proizvodna linija za presovanje oblog*

Test plates made of steel grade 235JR are prepared and three layers are overlay welded on each plate using electrodes with different coatings. The uneven surface layers are grinded. Test samples for the intended tests are cut out using water jet machine (Fig 2).

Pripremljene su ispitne ploče od čelika klase 235JR i tri sloja su navarena na svaku ploču pomoću elektrodama sa različitim oblogama. Neravni površinski slojevi se bruse. Ispitni uzorci za predviđena ispitivanja se izrezuju vodenim mlazom (Sl. 2).

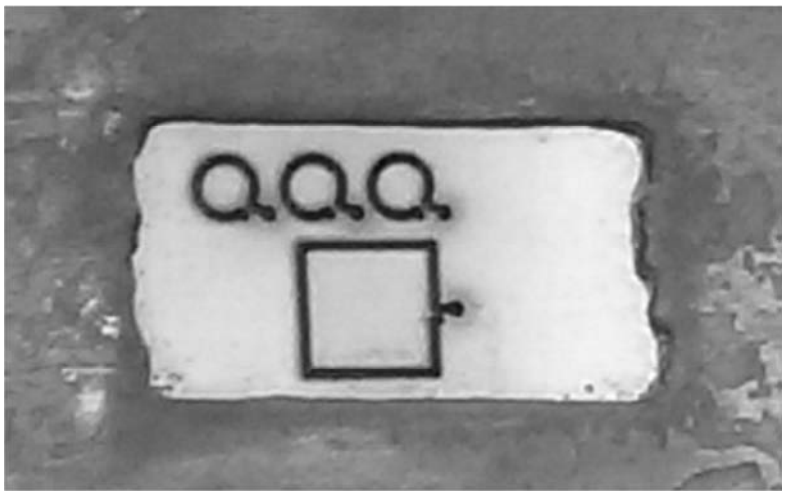

Figure 2 *Sample cutting scheme*
Slika 2. *Šema sečenja uzoraka*

Measurements of hardness HV15/15 and wear resistance of the overlay layer are carried out according to the methodology developed [5].

Results

Based on the experiments carried out it is found that the burning of the electrodes is very good and differs minimally from the reference electrodes E300. Only single cracks and imperfections are observed in the overlay metal at the highest concentrations of nano particles. The gradient of hardness of the overlay layers is represented as a ratio between the hardness of samples modified with nano particles and hardness of the base sample overlay welded using reference electrodes (Fig.3 и Fig.4).

Merenja tvrdoće HV 15/15 i otpornosti na habanje navarenog sloja izvode se prema razvijenoj metodologiji [5].

Rezultati

Na osnovu obavljenih eksperimenata utvrđeno je da je sagorevanje elektroda vrlo dobro i da se minimalno razlikuje od referentnih elektroda E300. U metalu navara uočene su samo pojedinačne prsline i nesavršenosti pri najvećim koncentracijama nanočestica. Gradijent tvrdoće navarenih slojeva predstavljen je odnosom između tvrdoće uzoraka modifikovanih nanočesticama i tvrdoće navara osnovnog uzorka navarenog referentnim elektrodama (Sl.3 i Sl.4).

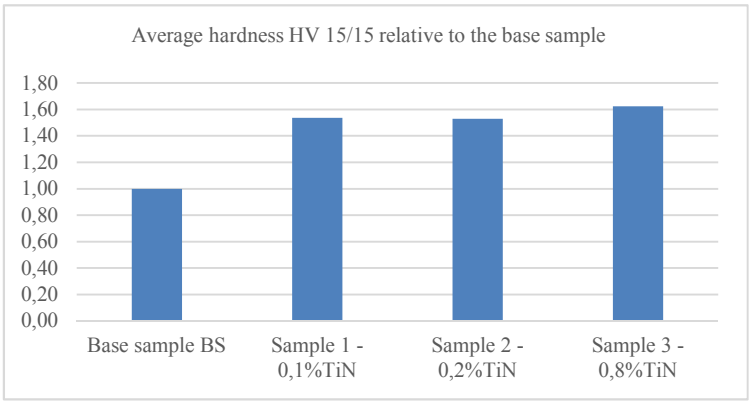

Figure 3. *Hardness gradient HV15/15 in dependence of TiN concentration*
Slika 3. *Gradijent tvrdoće HV15 / 15 u zavisnosti od koncentracije TiN*

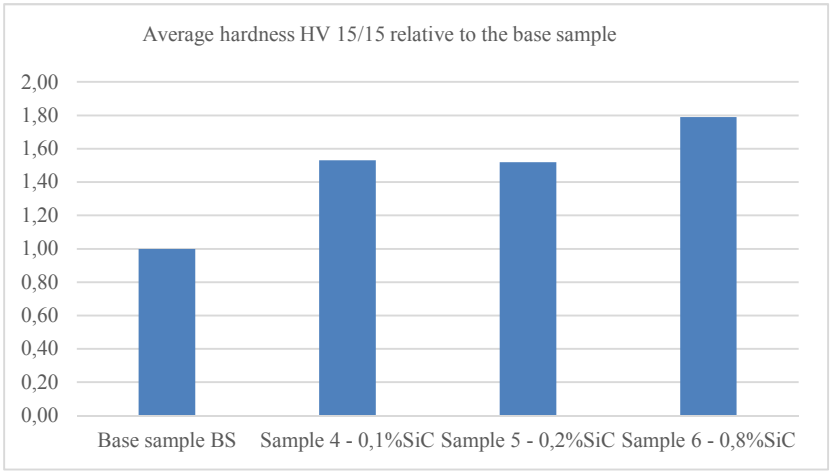

Figure 4. *Hardness gradient HV15/15 in dependence of SiC concentration*
Slika 4. *Gradijent tvrdoće HV15 / 15 u zavisnosti od koncentracije SiC*

The wear resistance gradient is also represented in comparison with the base sample (Fig. 5 and Fig. 6).

Gradijent otpornosti na habanje je takođe predstavljen u poređenju sa osnovnim uzorkom (Sl. 5 i Sl. 6).

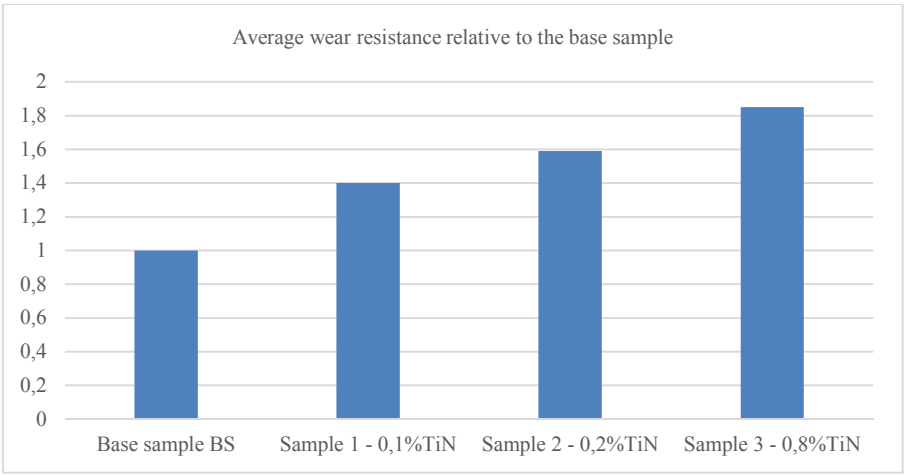

Figure 5. *Wear resistance gradient HV15/15 depending on TiN concentration*
Slika 5. *Gradijent otpornosti na habanje HV15 / 15 u zavisnosti od koncentracije TiN*

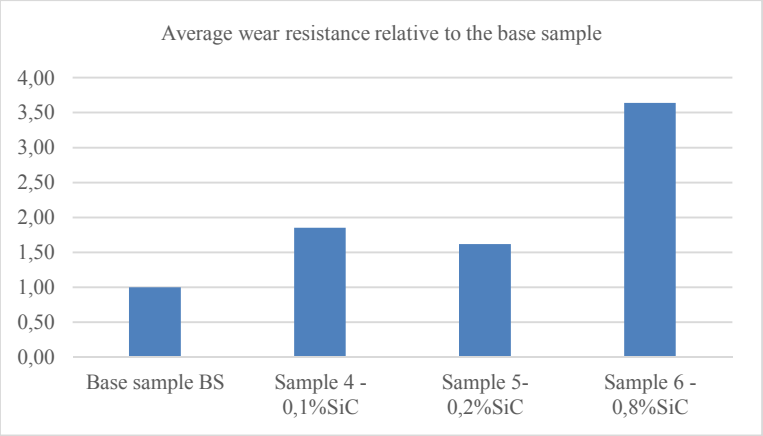

Figure 6. *Wear resistance gradient HV15/15 depending on SiC concentration*
Slika 6. *Gradijent otpornosti na habanje HV15 / 15 u zavisnosti od koncentracije SiC*

Metallography

The metallographic analysis is carried out on samples showing the best results for hardness and wear resistance. The surface of the samples is analyzed in state after overlay welding. For the purpose the surfaces of all samples are leveled through grinding to the same depth. The structure is developed according to the standard methodology. The metallographic analysis is carried out using microscope JENAVERT made by Carl Zeiss company. The results are shown in Table 1.

Metalografija

Metalografska analiza se obavlja na uzorcima koji pokazuju najbolje rezultate za tvrdoću i otpornost na habanje. Površina uzoraka se analizira u stanju posle navarivanja. U tu svrhu se površine svih uzoraka izravnavaju brušenjem do iste dubine. Struktura je razvijena prema standardnoj metodologiji. Metalografska analiza se radi pomoću mikroskopa JENAVERT kompanije Carl Zeiss. Rezultati su prikazani u Tabeli 1.

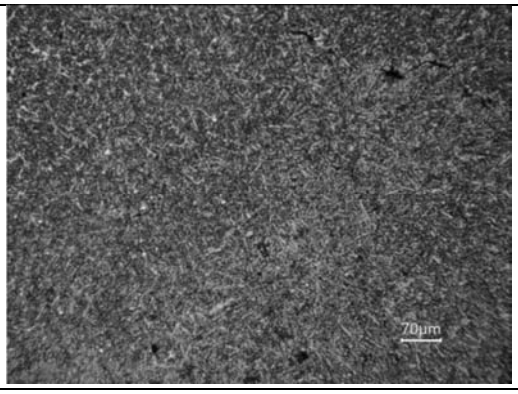

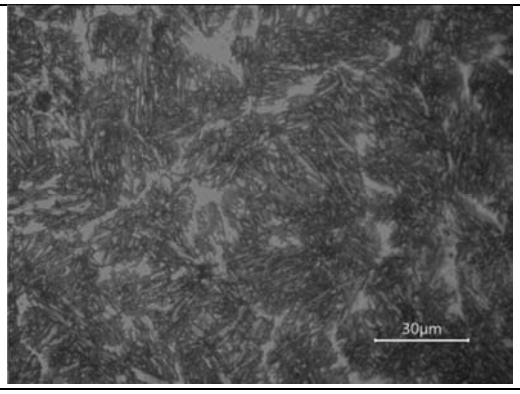

Base sample. The microstructure consists of rounded bainitic-martensitic areas confined by structurally free ferrite.
Osnovni uzorak. Mikrostruktura se sastoji od zaobljenih beinitno-martenzitnih područja omeđenih strukturalno slobodnim feritom

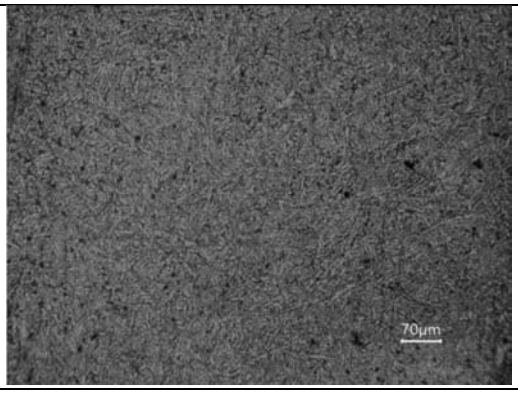

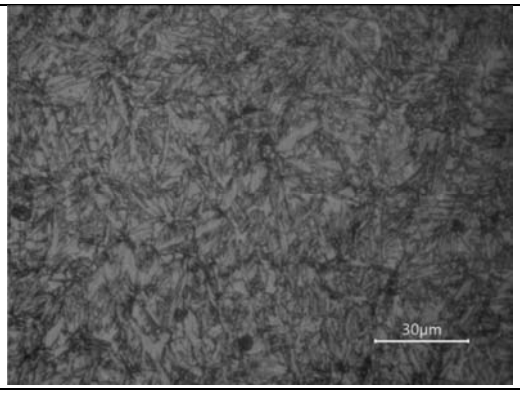

Sample 4. The microstructure is refined and homogenized and consists of fine bainite and structurally free ferrite.
Uzorak 4. Mikrostruktura je rafinisana i homogenizovana a sastoji se od finog beinita i strukturno slobodnog ferita

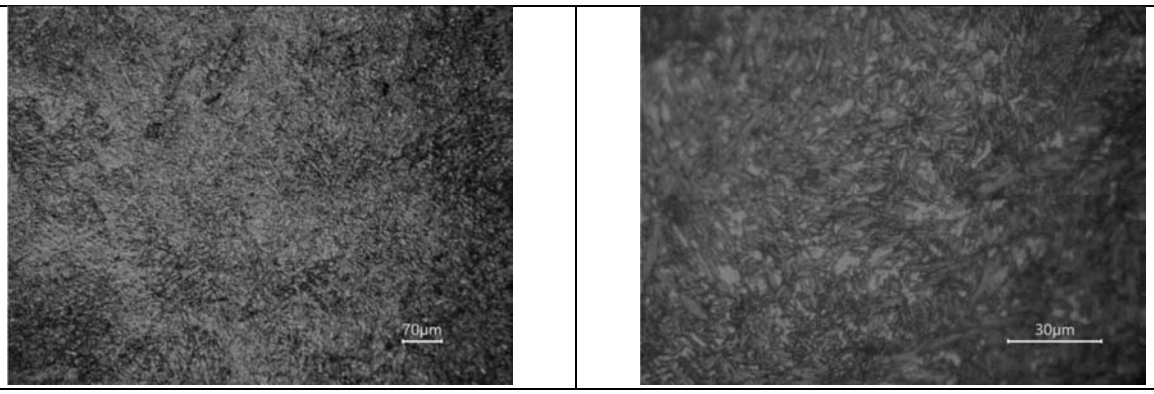

Sample 6. Grain refinement; the structure is bainitic-martensitic confined by structurally free ferrite.
Uzorak 6. Rafinacija zrna; struktura je beinitno-martenzitna ograničena strukturno slobodnim feritom.

Table 1. *Results from metallographic analysis*
Tabela 1. *Rezultati metalografske analize*

The microstructure is bainitic with different contents of martensite and ferrite. The presence of larger amount of pores is observed in the samples overlay welded with nano modified electrodes compared to the reference electrode. The pores affect the rate of cooling and crystallization of the overlay welded metal, which is probably the reason for formation of non-homogenized and non-uniform structure. This metallographic analysis cannot reveal obvious dependence between grain size and concentration of modifier. It is necessary to carry out an additional EBSD analysis (Electron BackScattered Diffraction) allowing making quantitative analysis in terms of grain size depending on their number in the area of a particular crystallographic plane. Such analysis is carried out [8] on samples of non-modified metal obtained with TIG welding. Determined is the distribution of the amount of grains depending on the diameter (per unit area) both for modified and non-modified structures (Fig. 6).

Mikrostruktura je beinitna sa različitim sadržajem martenzita i ferita. Prisustvo veće količine pora primećeno je na uzorcima koji su zavareni nano modifikovanim elektrodama u poređenju sa referentnom elektrodom. Pore utiču na brzinu hlađenja i kristalizacije navarenog metala, što je verovatno razlog za formiranje nehomogenizovane i neujednačene strukture. Ova metalografska analiza ne može otkriti očiglednu zavisnost između veličine zrna i koncentracije modifikatora. Potrebno je izvršiti dodatnu EBSD analizu (Electron Back Scattered Difraction-Difrakcija rasutim povratnim elektronima) koja omogućava kvantitativnu analizu u smislu veličine zrna u zavisnosti od njihovog broja u području određene kristalografske ravni. Takva analiza se radi [8] na uzorcima nemodifikovanog metala dobijenim TIG navarivanjem. Određena je raspodela količine zrna u zavisnosti od prečnika (po jedinici površine) kako za modifikovane tako i za ne-modifikovane strukture (Sl. 6).

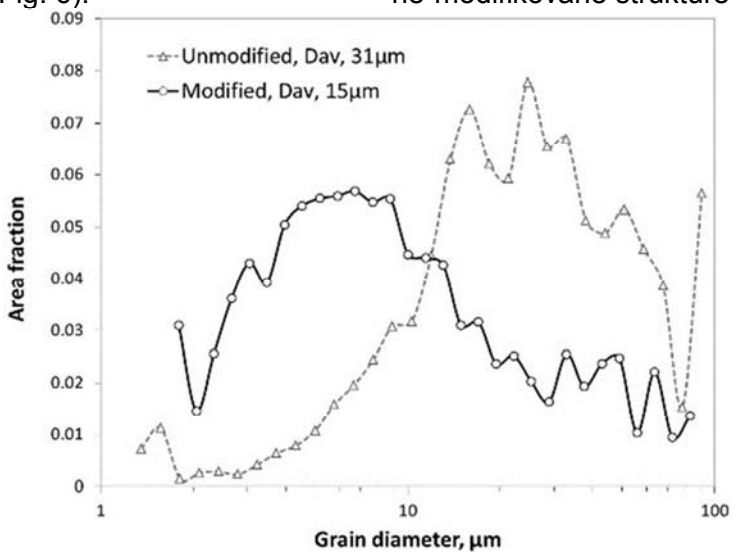

Figure 7. *Distribution of the average grain diameter (per unit area) in crystallographic planes for both modified and non-modified structures [8].*
Slika 7. *Distribucija prosečnog prečnika zrna (po jedinici površine) u kristalografskim ravninama za modifikovane i ne-modifikovane strukture [8].*

Conclusion

The introduction of nano size particles in the coating of electrodes for overlay welding grade E300 results in increase of hardness and wear resistance of the overlay layers manifested most distinctly in Sample 3 и Sample 6.

The metallographic analysis didn't find a distinct dependence between grain size and concentration of the modifier. It is necessary to carry out additional EBSD analisis.

In the future research, work should be done to reduce the formation of pores in the metal.

Zaključak

Uvođenje čestica nano veličine u sloj elektroda za navarivanje klase E300 rezultuje povećanjem tvrdoće i otpornosti na habanje nanetih slojeva, što se najviše manifestuje na uzorcima 3 i 6.

Metalografskom analizom nije pronađena razlika između veličine zrna i koncentracije modifikatora. Neophodno je obaviti dodatnu analizu EBSD-a.

U budućem istraživanju trebalo bi raditi na smanjenju stvaranja pora u metalu.

References

Reference

[1] Fattahi, M., N. Nabhani, M.R. Vaezi, E. Rahimi. Improvement of impact toughness of AWS E6010 weld metal by adding TiO2 nanoparticles to the electrode coating, Materials Science and Engineering A 528 (2011), pp.8031–8039.

[2] Fattahi, M., N. Nabhani, M.Hosseini, N. Arabian, E. Rahimi. Effect of Ti-containing inclusions on the nucleation of acicular ferrite and mechanical properties of multipass weld metals, Micron 45 (2013) pp.107–114.

[3] Antonov A.A., A.A.Artemev, G.N. Sokolov, I.V. Zorin, Y.N. Dubcov. 2015. "Effect of ultra-dispersed particles of TiN on the structure of overlay metal system Fe-Cr-C-Mo-Ni-Ti-B". Records of VolgGTU Ser. Problems of material science, welding and strength in Mechanical Engineering 168 (8). (in Russian)

[4] Sokolov G.N, I.V. Lysak, A.S. Troshkov, I.V. Zorin, S.S. Goremykina, A.V. Samohin, N.V. Alekseev, Y.V. Cvetkov. 2009. "Modifying the structure of the metal overlay welded with nano-dispersed tungsten carbides". Phisics and Chemistry of Material Processing (6): 41–47. (in Russian)

[5] P. Tashev, H. Kondov, E. Tasheva, M. Kandeva, „Study on hardness and wear resistance of layers overlayed using electrodes with nano-modified coating", International Journal of Engineering and Applied Sciences (EAAS); Islamabad, Pakistan, Vol 06. No. 04, 2015; pp 01 – 06, ISSN 2305-8269 [6] C. Vimalraj, P. Kah, B. Mvola and J. Martikainen "Effect of nanomaterial addition using GMAW and GTAW processes" Rev.Adv. Mater. Sci. 44 (2016) 370-382.

[7] P. Tashev, Ch. Kondov, Y. Lukarski, E. Tasheva, „Development of nano-modfied electrodes for manual arc welding, hardness of the overlay welded metal", Engineering Sciences, Year LII, 2015, № 3, scientific journal of BAS, p. 71, ISSN 1312-5702. (in Bulgarian)

[8] Tashev P., R. Lazarova, M. Kandeva, R. Petrov and V. Manolov, "Tungsten Inert Gas Weld Overlay using Nano-sized TiN Powder", JOURNAL OF THE BALKAN TRIBOLOGICAL ASSOCIATION, Vol. 22, No 3, 2238-2254, IF (2016).

[9] Petch N. J., Acta Metall., 34, 1387 (1986)

[10] Anchev V. C., Generalized "Strenght – Grain Size" Relationship, Max Planck Institute fur Metallforschung Stuttgart, Sonderseminar in Werkstoffkunde, 9. August 1994, Stuttgart

I.Voiculescu[1,a], V. Geanta[1,b], R. Stefanoiu[1,c], P. Vizureanu[2d], A.V.Sandu[2e], E.F.Binchiciu[3f]

The influence of alloying elements on the microstructure and microhardness of welded titanium alloys for medical applications

Uticaj legirajućih elemenata na mikrostrukturu i mikrotvrdoću zavarenih legura titana za medicinsku upotrebu

Originalni naučni rad / Original scientific paper

Rad je u izvornom obliku objavljen u Zborniku sa 4. IIW Kongresa zavarivanja Jugoistočne Evrope „Safe Welded Construction by High Quality Welding" održanog u Beogradu 10-13. Oktobra 2018

Rad primljen / Paper received:
Oktobar 2019.

Adresa autora / Author's address:
[1] University Politehnica of Bucharest, 313 Splaiul Independentei, 060042, Bucharest, Romania
[2]Technical University Gheorghe Asachi, Bd. Prof. Dimitrie Mangeron 67, 700050, Iași, Romania
[3] ISIM Timisoara, Mihai Viteazu 30, Timisoara, Romania
[a]ioneliav@yahoo.co.uk, [b]victorgeanta@yahoo.com, [c]radustefanoiu@yahoo.com, [d]peviz@tuiasi.ro, [e]sav@tuiasi.ro, [f]ebinchiciu@isim.ro

Ključne reči: legure titana, mikrostruktura, mikrotvrdoća

Key words: titanium alloys, microstructure, microhardness

Abstract

The paper presents the effects of some alloying elements (Al, Fe and Mn) on the microstructure and microhardness of titanium alloys that can be used for medical applications. The experimental alloys were produced by melting in an argon inert atmosphere of the RAV furnace, using high purity chemical elements and the commercial alloy Ti8Al4V. Were developed, under the same conditions, other binary alloys (Ti9Al, Ti5Fe, Ti3Mn, Ti6Mn) for highlighting the effects of the singular elements Al, Fe and Mn on the characteristics of titanium alloys. Microstructural analysis revealed the changes of microstructure produced by the introducing of alpha stabilizing elements (Al) or beta stabilizers (Fe, Mn). Were then analysed the effects of each type of chemical on the metal matrix microhardness and the density of the experimental alloys

Rezime

U radu su predstavljeni uticaji nekih legirajućih elemenata (Al, Fe i Mn) na mikrostrukturu i mikrotvrdoću titanovih legura koje se mogu koristiti u medicinske svrhe. Eksperimentalne legure su proizvedene topljenjem u peći sa inertnom atmosferom argona RAV, korišćenjem hemijskih elemenata visoke čistoće i komercijalne legure Ti8Al4V. Razvijene su, pod istim uslovima, druge binarne legure (Ti9Al, Ti5Fe, Ti3Mn, Ti6Mn) za isticanje uticaja pojedinih elemenata Al, Fe i Mn na karakteristike legura titana. Mikrostrukturna analiza je otkrila promene mikrostrukture nastale uvođenjem alfa stabilizirajućih elemenata (Al) ili beta stabilizatora (Fe, Mn). Zatim su analizirani efekti svake vrste hemikalija na mikrotvrdoću metalne matrice i gustinu eksperimentalnih legura.

1. Introduction

Some titanium alloys are getting much attention for biomaterials because they have excellent specific strength and corrosion resistance, no allergic problems and the best biocompatibility among metallic biomaterials [1]. Titanium's lightness and good mechano-chemical properties are salient features for implant applications [2]. Pure titanium and Ti-6Al-4V are still the most widely used ones for biomedical applications among the titanium biomaterials. For instance, the biocompatibility of Ti6Al4V alloy has since been called into question due to reports that the gradual release of aluminium, and particularly vanadium ions, from the surface of alloy can cause local adverse tissue reaction and immunological responses [1, 3 and 4]. Therefore, the developments of titanium alloys

1. Uvod

Neke legure titana dobijaju veliku pažnju kao biomaterijali jer imaju odličnu specifičnu čvrstoću i otpornost na koroziju, ne izazivaju alergijske probleme i najbolju biokompatibilnost među metalnim biomaterijalima [1]. Titanova lakoća i dobra mehano-hemijska svojstva su istaknute karakteristike za upotrebu kao implantata [2]. Čisti titan i legura Ti-6Al-4V i dalje su najčešće korišćeni za biomedicinsku primenu među titanovim biomaterijalima. Na primer, biokompatibilnost legure Ti6Al4V do tada je dovedena u pitanje zbog izveštaja da postepeno oslobađanje aluminijuma, a posebno jona vanadijuma, sa površine može izazvati lokalnu negativnu reakciju tkiva i imunološke reakcije [1, 3 i 4]. Stoga su izraziti zahtevi za razvoj legura titana za biomedicinsku

targeted for biomedical application are highly required. Recently, mechanical biocompatibility of biomaterials is regarded as important factor, and therefore the research and development of β types titanium alloys, which are advantageous from that point, are increasing [1]. The β type titanium alloys show excellent cold workability and high strength. The strength of β type titanium alloys can be increased with keeping Young's modulus low by cold working after solution treatment even the elongation and reduction area are a little lowered at low cold work ratio by around 20% [1]. A low Young's modulus equivalent to that of cortical bone is simultaneously required in order to inhibit bone absorption into the implant [5, 6 and 7].

The elements which are judged to be non-toxic and non-allergenic through the reported data of cell viability for pure metals, polarization resistance and tissue compatibility, that can be used as alloying elements are: Nb, Ta, Zr, Sn, Mo, Fe, Hf. Stabilisation of titanium alloys using different alloying elements, for the α-phase (e.g. Al, O) and for β-phase (V, Fe, Mn, Nb, Ta), is a current practice. At a content of more 5wt%aluminium the precipitation of Ti_3Al in the α_2-phase begins, as can be seen from the quasi-binary section in the ternary phase diagram of Ti6Al4V. The α_2-phase provides an extremely high hardening effect so that the aluminium content in titanium alloys must be limited to a maximum value of 8% [8]. Also, grain size of as cast titanium alloy decreases significantly with boron addition [9]. The β phase field extends to higher aluminium contents and the width of the α+β two phase region is very narrow, less than 1at% Al. During recent efforts to develop TiAl-base alloys for structural applications only little information has gained on the effect of Fe additions on the mechanical properties [10]. The solid solubility for Fe in all Al-Ti phases is very limited. The maximum content of Fe in αTi is about 1at% at an Al content of 44 at% [11]. Aluminium addition increases the β transus, raising either a eutectoid ($\beta \rightarrow \alpha + Ti_5Si_3$) or peritectoid ($\beta + Ti_5Si_3 \rightarrow \alpha$) reaction temperature in the ternary system [12]. Manganese reduces the α2-Ti3Al level, but otherwise its behaviour is similar to a standard Ti-8Al type alloy [13]. The addition of Mn in Ti has depressed the transformation temperature from α to β phase. The influence of manganese on transition temperature is significant and it is confirmed that the Mn is a β stabilizing addition element for Ti metals. The hardness increased significantly ranging from 83.3GPa (Ti2Mn) to 122GPa (Ti12Mn) and the ductility decreased ranging from 21.3% to 11.7% with

primenu. U poslednje vreme, mehanička biokompatibilnost biomaterijala smatra se važnim faktorom i zato se istraživanje i razvoj legura titana tipa β koje imaju prednost sa te tačke gledišta, povećava [1]. Titanove legure tipa β pokazuju odličnu obradivost na hladno i visoku čvrstoću. Ćvrstoća legura titana tipa β može se povećati održavanjem Jungovog modula niskim, hladnom obradom posle rastvarajućeg tretmana, čak i izduženje i suženje postaju malo smanjeni pri obradi na hladno za oko 20% [1]. Istovremeno je potreban nizak Jungov modul ekvivalentan kortikalnoj kosti da bi se inhibirala apsorpcija kostiju u implantat [5, 6 i 7].

Elementi za koje se zna da su netoksični i nealergenski, zbog objavljenih podataka o ćelijskoj održivosti čistih metala, polarizacijskoj otpornosti i kompatibilnosti tkiva, te se mogu koristiti kao legirajući elementi su: Nb, Ta, Zr, Sn, Mo, Fe, Hf. Stabilizacija titanovih legura korišćenjem različitih legirajućih elemenata, za α-fazu (npr. Al, O) i -β fazu (V, Fe, Mn, Nb, Ta), je trenutna praksa. Sa sadržajem više od 5 mas.% aluminijuma, počinje taloženje Ti_3Al u α_2-fazi, kao što se može videti iz kvazi-binarnog preseka u trojnom faznom dijagramu Ti6Al4V. α_2-faza daje izuzetno visok efekat otvrdnjavanja tako da sadržaj aluminijuma u titanovim legurama mora biti ograničen na maksimalnu vrednost od 8% [8]. Takođe, veličina zrna livene legure titana značajno se smanjuje dodatkom bora [9]. Fazno polje β se proširuje pri većem sadržaju aluminijuma i širina α+β dvofazne oblasti je vrlo uska, manja od 1at% Al. Tokom nedavnih napora za razvojem legura na bazi TiAl za konstrukcionuu primenu, stečeno je malo informacija o uticaju dodataka Fe na mehanička svojstva [10]. Rastvorljivost u čvrstom stanju za Fe u svim Al-Ti fazama je vrlo ograničena. Maksimalni sadržaj Fe u αTi je oko 1at%, a sadržaj Al 44 od 44%% [11]. Dodavanje aluminijuma povećava β , podižući temperature ili eutektoidne ($\beta \rightarrow \alpha + Ti_5Si_3$) ili peritektoidne ($\beta + Ti_5Si_3 \rightarrow \alpha$) reakcije u trojnom sistemu [12].

Mangan smanjuje nivo α2-Ti3Al, ali inače je njegovo ponašanje slično standardnoj leguri tipa Ti-8Al [13]. Dodavanje Mn u Ti je smanjilo temperaturu transformacije iz α u β fazu. Uticaj mangana na temperaturu prelaska je značajan i potvrđeno je da je Mn β- stabilizujući dodatni element za Ti metale. Tvrdoća se značajno povećala u rasponu od 83,3GPa (Ti2Mn) do 122GPa (Ti12Mn), a duktilnost se smanjila u rasponu od 21,3% do 11,7% sa povećanjem sadržaja mangana u Ti [14]. Intoksikacije metalnim

increasing manganese content in Ti [14]. Intoxications with metallic aluminium are recognised in occupational medicine and in patients submitted to renal dialysis. Since the disease has been linked to a generic defect, aluminium is considered to play a minor role in the onset of Alzheimer's disease [15 and 16]. Iron is biologically omnipresent essential element. Iron is toxic only after extremely high levels of exposure. Iron released by oxidation process does not accumulate in tissues and is immediately metabolised [16]. By restricting grain growth, iron help in formation of fine grained microstructures in titanium alloy. Manganese has no toxic effect except after extreme occupational exposure. It is an essential element and plays a primary role in the activation of multiple enzyme systems [16, 17 and 18]. Manganese is also beneficial to the normal skeletal growth and development. In recent decades research has discovered the special role of manganese plays as a co-factor in the formation of bone cartilage and bone collagen, as well as in bone mineralization [14 and 19]. Beta Ti alloys are most versatile class of Ti alloys offering a wide range of processing and physical-chemical and mechanical properties combinations compared with any other class of Ti alloys [20]. Also, Beta -Ti alloys can be strengthened by heat treatment. The hardness and the elastic modulus increased significantly by increasing the manganese content in the Ti metallic matrix from 2wt.%Mn to 12 wt.% Mn, but the ductility decreased from 21.3wt.% (Ti2Mn) to 11.7wt.% (Ti12Mn). Concentrations of Mn below 8 wt. % in titanium reveal negligible effects on the metabolic activity and the cell proliferation of human osteoblasts [21, 22]. In conclusion, iron and manganese additions are likely to enhance the nucleation rate by providing additional driving force and/or slowing the growth rate by influencing the liquid/solid interfacial characteristics [23]. In the present study there are considering the effects of the elements Al, Fe and Mn on the microstructure and microhardness of titanium alloys for medical applications. Aluminium stabilizes the alpha phase in titanium alloy, having the lamellar appearance, for the content of below 8 wt. % Al. Iron increases the relative density of the alloy and forms three types of compounds. The chemical elements that substantially increases the microhardness of titanium alloy was Fe and Al, if these are introduced simultaneously (634 HV0.1 for Ti8Al5Fe) or singular (502 HV0.1 for Ti5Fe). Effect of Mn on the increasing of hardness is less important, yielding a slight increase of microhardness from 418HV0.1 for Ti3Mn to 427HV0.1 for Ti5.7Mn.

aluminijumom prepoznate su u medicini rada i kod pacijenata koji su podvrgnuti bubrežnoj dijalizi. Pošto je bolest povezana sa generičkim oštećenjem, smatra se da aluminijum igra manju ulogu u nastanku Alzheimerove bolesti [15 i 16]. Gvožđe je biološki sveprisutni esencijalni element. Gvožđe je toksično samo nakon izuzetno visokog nivoa izloženosti. Gvožđe oslobođeno procesom oksidacije ne akumulira se u tkivima i odmah se metabolizuje [16]. Ograničavanjem rasta zrna, gvožđe pomaže u stvaranju sitnozrnate mikrostrukture u leguri titana.

Mangan nema toksično dejstvo osim nakon ekstremnog profesionalnog izlaganja. To je suštinski element i igra primarnu ulogu u aktiviranju više enzimskih sistema [16, 17 i 18]. Mangan je takođe koristan za normalan rast i razvoj skeleta. U poslednjim decenijama istraživanje je otkrilo posebnu ulogu mangana koji je ko-faktor u stvaranju koštane hrskavice i koštanog kolagena, kao i u mineralizaciji kostiju [14 i 19]. Beta Ti legure su najsvestranija klasa Ti legura koje nude širok spektar kombinacija prerade i fizičko-hemijskih i mehaničkih svojstava u poređenju sa bilo kojom drugom klasom Ti legura [20]. Takođe, Beta-Ti legura mogu se ojačati termičkom obradom. Tvrdoća i modul elastičnosti značajno su porasli povećavanjem sadržaja mangana u Ti metalnoj matrici sa 2 tež.% Mn na 12 tež.% Mn, ali duktilnost se smanjila sa 21.3 tež.% (Ti2Mn) na 11.7 tež.%. Koncentracije Mn ispod 8 tež. % u titanu otkriva zanemarljive efekte na metaboličku aktivnost i ćelijsku proliferaciju ljudskih osteoblasta [21, 22].

Zaključno, dodaci gvožđa i mangana verovatno će povećati brzinu nukleacije pružajući dodatnu pokretačku silu i / ili usporavajući brzinu rasta uticajem na tečne / čvrste interfacijalne karakteristike [23]. U ovom istraživanju razmatraju se uticaji elemenata Al, Fe i Mn na mikrostrukturu i mikrotvrdoću titanovih legura za medicinske primene. Aluminijum stabilizuje alfa fazu u leguri titana, koji ima lamelarni izgled, za sadržaj ispod 8 tež. % Al. Gvožđe povećava relativnu gustinu legure i formira tri vrste jedinjenja. Hemijski elementi koji značajno povećavaju mikrotvrdoću legure titana bili su Fe i Al, ako se uvode istovremeno (634 HV0.1 za Ti8Al5Fe) ili pojedinačno (502 HV0.1 za Ti5Fe). Uticaj Mn na povećanje tvrdoće je manje važan, što dovodi do blagog porasta mikrotvrdoće sa 418HV0.1 za Ti3Mn na 427HV0.1 za Ti5.7Mn.

2. Experimental details

2.1 Obtaining of new titanium alloys

The experimental alloys were produced by melting in an argon inert atmosphere of the RAV installation, using high purity metallic materials and the commercial alloy Ti8Al4V. Under the same conditions, other binary alloys (Ti9Al, Ti5Fe, Ti3Mn and Ti6Mn) has been obtained for highlighting the effects of the singular elements Al, Fe and Mn on the characteristics of titanium alloys. The alloys composition was conducted from a trade mark alloys (Ti8Al4V), and subsequently 6 experimental titanium alloys were obtained, by changing the content of chemical elements like Fe, Mn and Al. These alloys were developed as a basis of comparison for the study of the singular effects of alloying elements Al, Fe and Mn. Chemical composition of the alloys obtained in this study, determined by spectrophotometry, is presented in Table 1.

2. Detalji eksperimenta

2.1 Dobijanje novih legura titana

Eksperimentalne legure su proizvedene topljenjem u inertnoj atmosferi argona RAV instalacije, korišćenjem metalnih materijala visoke čistoće i komercijalne legure Ti8Al4V. Pod istim uslovima, druge binarne legure (Ti9Al, Ti5Fe, Ti3Mn i Ti6Mn) su dobijene za isticanje uticaja pojedinih elemenata Al, Fe i Mn na karakteristike titanovih legura. Sastav legura je izveden iz legura trgovačke marke (Ti8Al4V), a zatim je dobijeno 6 eksperimentalnih legura titanijuma, promenom sadržaja hemijskih elemenata poput Fe, Mn i Al. Ove legure su razvijene kao osnova za upoređivanje za proučavanje pojedinačnih efekata legirajućih elemenata Al, Fe i Mn. Hemijski sastav legura dobijenih u ovom istraživanju, određen spektrofotometrijom, prikazan je u Tabeli 1.

Sample Uzorak	Chemical elements (wt.%) Hemijski elementi (tež.%)					
	Mn	Fe	Al	V	Sn	Ti
Ti8Al4V trade mark	0.03	0.03	8.26	2.44	0.82	Bal.
Ti8Al	0.16	0.11	8.4	0.04	0.8	
Ti8Al2.8Fe	0.16	2.85	8.35	0.04	0.82	
Ti9Al5Fe	0.07	5.1	9.35	0.04	0.78	
Ti5Fe	0.07	4.9	0.06	0.04	0.78	
Ti5.7Mn	5.77	0.11	0.06	0.04	0.94	
Ti3Mn	3.07	0.10	0.06	0.04	0.72	

Table 1. *Chemical composition of new titanium alloys*
Tabela 1. *Hemijski sastav novih legura titana*

2.2 Welding of new titanium alloys

The mechanical properties of the welded titanium alloys depend on the structural characteristics of each welding zone, which in turn depends on the thermal cycles during welding and heat treatments. The fusion zone for titanium alloys is characterized by the presence of β-phase, which forms columnar grains during solidification at welding. The size and morphology of these grains depending on the heat flow loss during welding solidification. Although the welding procedures and equipment used for austenitic stainless steel and aluminium alloys can be applied in order to join commercially pure titanium and most of titanium alloys, their increased reactivity with atmospheric elements at high temperatures necessitates additional precautions to shield the molten weld pool. The titanium interacts actively with atmospheric gases, such as oxygen,

2.2 Zavarivanje legura titana

Mehanička svojstva zavarenih legura titana zavise od strukturnih karakteristika svake zone zavarivanja, što zavisi od toplotnih ciklusa tokom zavarivanja i termičke obrade. Zonu stapanja za legure titana karakteriše prisustvo β -faze koja formira stubičasta zrna tokom očvršćavanja pri zavarivanju. Veličina i morfologija ovih zrna zavisi od gubitka toplotnog protoka tokom očvršćavanja. Iako se postupci zavarivanja i oprema koja se koristi za austenitni nerđajući čelik i legure aluminijuma mogu primeniti kod komercijalno čistog titana i većine titanovih legura, njihova povećana reaktivnost sa atmosferskim elementima na visokim temperaturama zahteva dodatne mere predostrožnosti kako bi se zaštitila zavarivačka kupka. Titan aktivno stupa u interakciju sa atmosferskim gasovima, kao što su kiseonik, vodonik, azot tokom zagrevanja iznad 350 ^{o}C, što

hydrogen, nitrogen during the heating more than 350 ^{o}C, conducting to decrease of the weld mechanical properties. Titanium alloys are sensitive to thermal cycle due to a heavy increase of grains during heating and cooling in the area of β phase. Therefore, during welding a minimum heat input value must be chosen. The main welding processes that can be used for joining titanium alloys are: TIG and MIG welding, friction welding, electron beam welding and laser welding [25 and 26].

The paper presents the effects of some alloying elements (Al, Fe and Mn) on the microstructure and microhardness of titanium alloys that was welded using GTAW process. The Ti-based experimental alloys were welded by TIG welding by simultaneously melting the ends of the overlapping samples without filler material, given the relatively small dimensions of the parts. The Ti6Al4V alloy 1.6 mm-thick samples were welded using the TIG process and Ti6Al4V filler material 1.6mm-thick, using a welding device that provided the inert shielding gas to the welded root. The values of welding parameters were: welding current, Is = 20A; arc voltage, Ua = 10V; Welding Gas flow = 12l/min; Root Gas flow = 5 l/min. After welding, the samples were cut and the cross sections were prepared for microstructural analyses (fig. 1).

dovodi do smanjenja mehaničkih svojstava spoja. Legure titana su osetljive na toplotni ciklus zbog velikog povećanja zrna tokom zagrevanja i hlađenja u oblasti β faze. Zbog toga se tokom zavarivanja mora odabrati minimalna vrednost unosa toplote. Glavni postupci zavarivanja koji se mogu koristiti za spajanje legura od titana su: TIG i MIG zavarivanje, zavarivanje trenjem , zavarivanje elektronskim snopom i laserom [25 i 26].

U radu su prikazani uticaji nekih legirajućih elemenata (Al, Fe i Mn) na mikrostrukturu i mikrotvrdoću titanovih legura koji su zavareni postupkom TIG. Eksperimentalne legure na bazi Ti su zavarene TIG zavarivanjem istovremeno topljenjem krajeva uzoraka koji se preklapaju bez dodatnog materijala s obzirom na relativno male dimenzije delova. Uzorci od legure Ti6Al4V su 1,6 mm debljine, zavareni TIG postupkom i Ti6Al4V dodatni materijal debljine 1,6 mm, koristeći uređaj koji je obezbedio zaštitu inertnim gasom zavarenog korena. Vrednosti parametara zavarivanja bile su: struja zavarivanja, Is = 20A; napon, Ua = 10V; protok zavarivačkog gasa = 12l / min; protok gasa za zaštitu korena = 5 l / min. Nakon zavarivanja, uzorci su isečeni i poprečni preseci pripremljeni su za mikrostrukturne analize (slika 1).

a) *b)*

Figure 1. *Cross sections through welded samples: a)Ti5Fe alloy; b) Ti3Mn alloy*
Slika 1. *Poprečni preseci zavarenih uzoraka a)Ti5Fe legura; b) Ti3Mn a)Ti5Fe alloy; b) Ti3Mn alloy*

3. Results

3.1 Microstructure

For metallographic analysis the samples were precision cutting and then were subsequently embedded in resin and polished using metallographic paper with different grain sizes (600 to 2500 grit paper) and abrasive paste (grain size between 0.6 to 0.1 μm). Metallographic etching reagent was used with the following composition: 10% HF + 30% HNO3 + 50ml deionized water. The samples were examined by optical microscopy (Olympus GX51 optical microscope).

In the case of the commercial Ti8Al4V alloy processed by rolling we can observe very fine grain and orientated in strings (figure 2). After remelting, the microstructure is dendritic, with clear differentiation of the aluminium-rich phase, α phase

3. Rezultati

3.1 Mikrostruktura

Za metalografske analize, uzorci su precizno sečeni, a zatim su ugrađeni u smolu i polirani etalografskim papirom različitih veličina zrna (papir od 600 do 2500 grit) i brusne paste (veličina zrna između 0,6 do 0,1 μm). Upotrebljen je metalografski reagens za nagrizanje sledećeg sastava: 10% HF + 30% HNO3 + 50 ml dejonizovane vode. Uzorci su ispitani optičkom mikroskopom (Olimpus GKS51 optički mikroskop). U slučaju komercijalne legure Ti8Al4V dobijene valjanjem možemo primetiti vrlo fino zrno i orijentisano u nizovima (slika 2). Posle pretapanja, mikrostruktura je dendritna, sa jasnom diferencijacijom faze bogate aluminijumom, α faze i Ti3Al faze. Sistem Ti-Al uključuje sledeća jedinjenja: TiAl (kongruentan, tačka topljenja 1733

and Ti3Al phase. The system Ti-Al includes the following compounds: TiAl (congruent, melting point 1733 K), $TiAl_3$ (congruent, melting point 1613 K), Ti_3Al, $TiAl_2$ and Ti_2Al_5 (incongruent). The compounds TiAl and $TiAl_3$ are the most stable [17, 18].

K), TiAl3 (kongruentan, tačka topljenja 1613 K), Ti3Al, TiAl2 i Ti2Al5 (inkoguentno). Jedinjenja TiAl i TiAl3 su najstabilnija [17, 18].

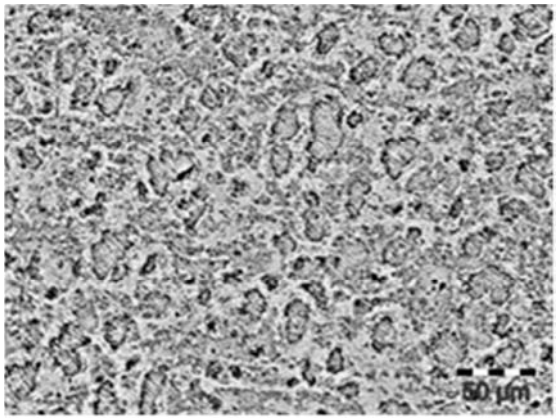

Figure 2. *Microstructure of commercial Ti8Al4V alloy*
Slika 2. *Mikrostruktura komercijalne Ti8Al4V legure*

The addition of 6 wt% aluminium to the CP titanium did not change the as-cast microstructure, and this is in correlation to the fact that aluminium has a very high solid solubility in titanium [24].

For 9 wt% Al addition or more, in conformity with the Ti-Al phase diagram, some intermetallic second phase can form (Ti_3Al) (figure 3). TiAl based materials are pursued mainly because of their high thrust-to-weight ratio of high –performance aircraft engines.

The microstructure of these alloys can be controlled by heat treatment. The optimum desirable properties in this class of alloys could be achieved only with (α_2+γ) microstructure, which corresponds to the composition Ti48Al [2].

Dodavanje 6 tež.% aluminijuma u CP titan nije promenilo mikrostrukturu livenog materijala, a to je u korelaciji sa činjenicom da aluminijum ima veoma visoku rastvorljivost u čvrstom stanju titana [24].

Za dodavanje 9 tež% Al ili više, u skladu sa faznim dijagramom Ti-Al, može se formirati neka intermetalna druga faza (Ti3Al) (slika 3). TiAl materijali traženi su uglavnom zbog visokog odnosa snage i težine kod motora aviona visokih performansi.

Mikrostruktura ovih legura može se kontrolisati termičkom obradom. Optimalna poželjna svojstva u ovoj klasi legura mogu se postići samo (α_2+γ) mikrostrukturom, što odgovara sastavu Ti48Al [2].

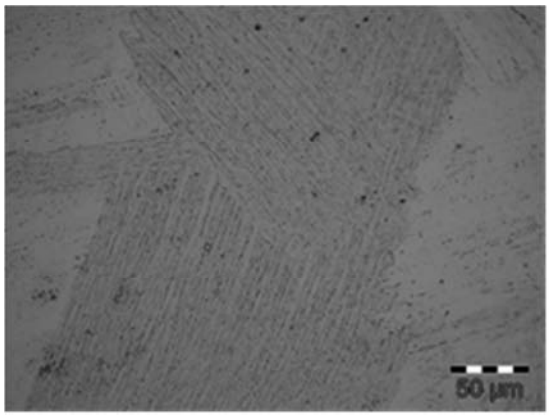

Figure 3. *Microstructure of experimental Ti8Al alloy*
Slika 3. *Mikrostruktura eksperimentalne legure Ti8Al*

The addition of 2.8% Fe in the alloy Ti8Al promotes the change of β phase proportion, although alpha phase is still predominant (figure 4). The specific aspect of metallic matrix is lamellar, with dispersed particles of intermetallic compounds (Ti3Al), both in base material and weld (figure 5).

Dodavanje 2,8% Fe u leguri Ti8Al pospešuje promenu udela β faze, iako alfa faza i dalje preovlađuje (slika 4). Specifični aspekt metalne matrice je lamelarni, sa raspršenim česticama intermetalnih jedinjenja (Ti3Al), kako u osnovnom materijalu, tako i u šavu (slika 5).

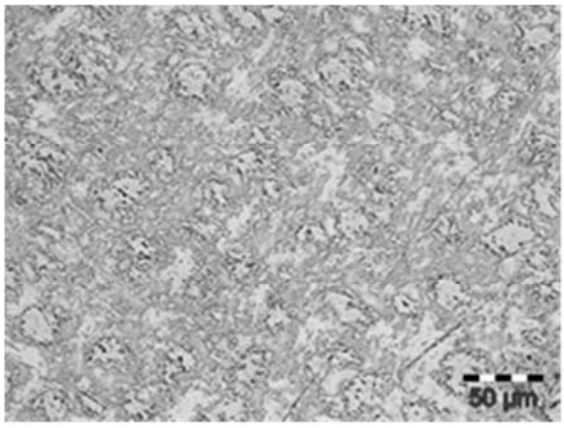

Figure 4. *Microstructure of experimental Ti8Al2*
Slika 4*. Mikrostruktura eksperimentalne legure Ti8Al2*

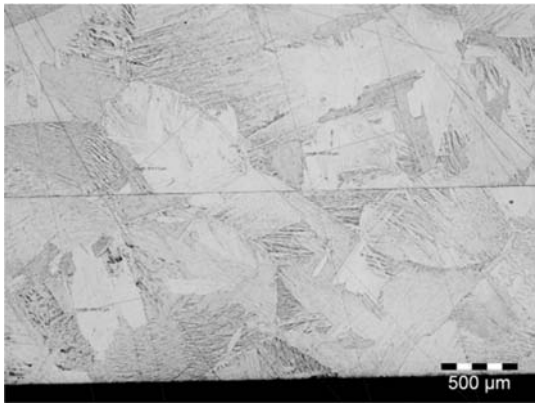

Figure 5. *Microstructure of weld for T8Al2 alloy*
Slika 5. *Mikrostruktura šava kod legure Ti8Al2*

Analysing Ti-Fe system, we can conclude that this alloy includes the following compounds: TiFe2 (congruent, melting point at 1700 K), TiFe (incongruent, melting point at 1650 K), Ti2Fe (incongruent, melting point at 1358 K). The most stable compound is TiFe2 [17, 19]. Increasing of Fe content up to 5 wt% in the alloy metal matrix Ti8Al no reveal any substantial change of the microstructure in terms of the types of existing phases (figure 6).

It notes, however, a spheroidization tendency and grain finishing compound TiFe2, with average diameter value of 25 µm in the case of the alloy with 2.5%wt Fe, to about 15 µm in the case of alloy having 5%wt Fe.

Analizirajući sistem Ti-Fe, možemo zaključiti da ova legura uključuje sledeća jedinjenja: TiFe2 (kongruentna, tačka topljenja na 1700 K), TiFe (inkongruentna, tačka topljenja 1650 K), Ti2Fe (inkoguentna, tačka topljenja na 1358 K). Najstabilnije jedinjenje je TiFe2 [17, 19]. Povećanje sadržaja Fe do 5 mas.% u matrici legiranog metala Ti8Al ne otkriva značajne promene mikrostrukture u smislu vrsta postojećih faza (slika 6).

Međutim, primećuje se tendencija sferoidizacije i završavanja zrna jedinjenja TiFe2, prosečne vrednosti prečnika od 25 µm u slučaju legure sa 2,5 mas.% Fe, do oko 15 µm u slučaju legure sa 5 mas.% Fe.

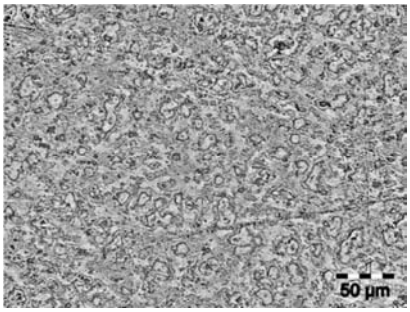

Figure 6. *Microstructure of experimental Ti9Al5Fe alloy*
Slika 6. *Mikrostruktura eksperimentalne legure Ti9Al5Fe*

The intermetallic compounds TiFe2 are relatively uniform dispersed into metallic matrix of Ti5Fe alloy (figure 7).

Intermetalna jedinjenja TiFe2 su relativno jednoliko dispergovana u metalnoj matrici legure Ti5Fe (slika 7).

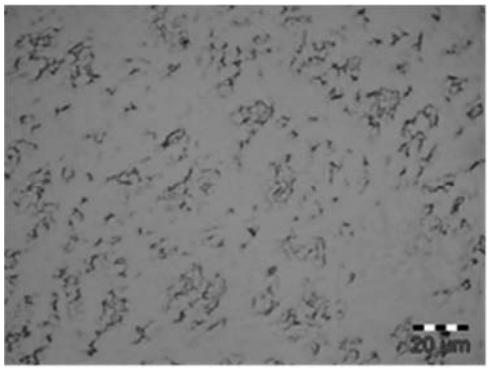

Figure 7. *Microstructure of Ti5Fe alloy*
Slika 7. *Mikrostruktura legure Ti5Fe*

Increasing the Fe content in titanium above the maximum solubility value has led to the separation of some compounds on the grain boundaries of the weld (figure 8).

Povećanje sadržaja Fe u titanu iznad maksimalne vrednosti rastvorljivosti, dovelo je do izdvajanja nekih jedinjenja na granicama zrna u šavu (slika 8).

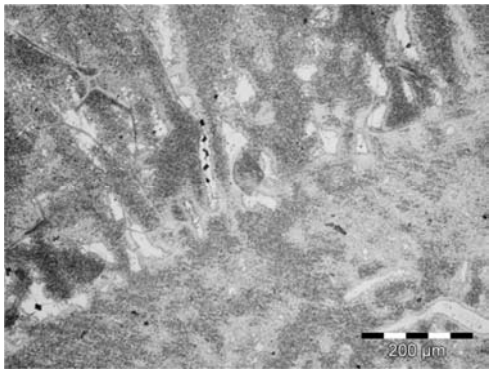

Figure 8. *Microstructure of weld and heat affected zone for Ti5Fe alloy*
Slika 8. *Mikrostruktura šava i zone uticaja toplote kod legure Ti5 Fe*

By alloying titanium with Mn, phase stabilization is achieved, with uniform equiaxed grains β (figure 9).
The Mn could be used in lower concentrations as an alloying element for biomedical titanium.
The Ti2Mn, Ti5Mn, and Ti8Mn alloys with good mechanical properties and acceptable cytocompatibility have a potential for use as bone substitutes and dental implants [23].

Legiranjem titana sa Mn postiže se fazna stabilizacija, sa ravnomerno izjednačenim β zrnima (slika 9).
Mn se može koristiti u nižim koncentracijama kao legirajući element za biomedicinski titan.
Legure Ti2Mn, Ti5Mn i Ti8Mn sa dobrim mehaničkim svojstvima i prihvatljivom cito-kompatibilnošću mogu se koristiti kao zamena za kosti i kao zubni implantat [23].

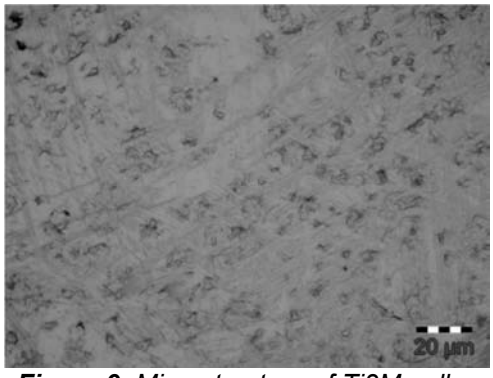

Figure 9. *Microstructure of Ti3Mn alloy*
Slika 9. *Mikrostruktura legure Ti3Mn*

Further increasing of Mn content (5.7%wt Mn) increases the proportion of intermetallic compounds that will separate into the metallic matrix having fine and lamellar aspect, even into base material (figure 10) and weld (figure 11).

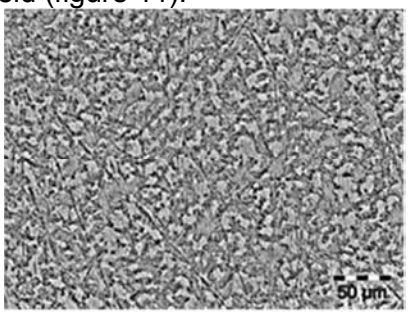

Figure 10. *Microstructure of experimental Ti5.7Mn*
Slika 10. *Mikrostruktura eksperimentalne legure Ti5,7 Fe*

Daljnjim povećanjem sadržaja Mn (5,7 mas.% Mn) povećava se udeo intermetalnih jedinjenja koja će se odvojiti u metalnu matricu koja ima fini i lamelarni oblik, čak i u osnovni materijal (slika 10) i šav (slika 11).

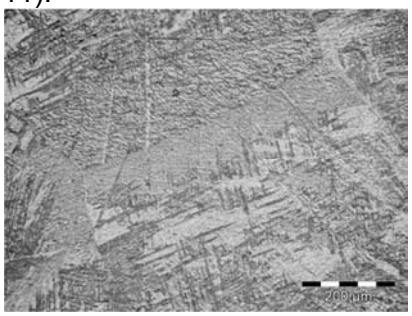

Figure 11. *Microstructure of weld for Ti5.7Mn alloy*
Slika 11. *Mikrostruktura šava kod legure Ti5.7Mn*

3.2 Microhardness

The general trend of the increase in hardness for the TiFe and TiMn alloys can be explained by solid solution strengthening mechanism. When the titanium lattice is disorder by substitutional solid solution additions, it becomes strained or there is an increase in internal energy of the system due to lattice straining caused by an increase in amount of the doping element which results in localized straining on substitutional sites [23 and 24]. The average values of microhardness, measured using a Shimadzu HMV 2T apparatus in 10 different points of the alloys analysed in this paper, are shown in Figure 12.

3.2 Mikrotvrdoća

Opšti trend povećanja tvrdoće za TiFe i TiMn legure može se objasniti mehanizmom ojačavanja rastvaranjem. Kada je rešetka titana poremećena dodavanjem supstitucionih čvrstih rastvora, ona postaje deformisana ili dolazi do povećanja unutrašnje energije sistema usled deformacije rešetke izazvane povećanjem količine “doping” elementa što dovodi do lokalizovane deformacije na mestu zamene [23 i 24]. Prosečne vrednosti mikrotvrdoće, merene uređajem Shimadzu HMV 2T u 10 različitih tačaka na analiziranim legurama u ovom radu, prikazane su na slici 12.

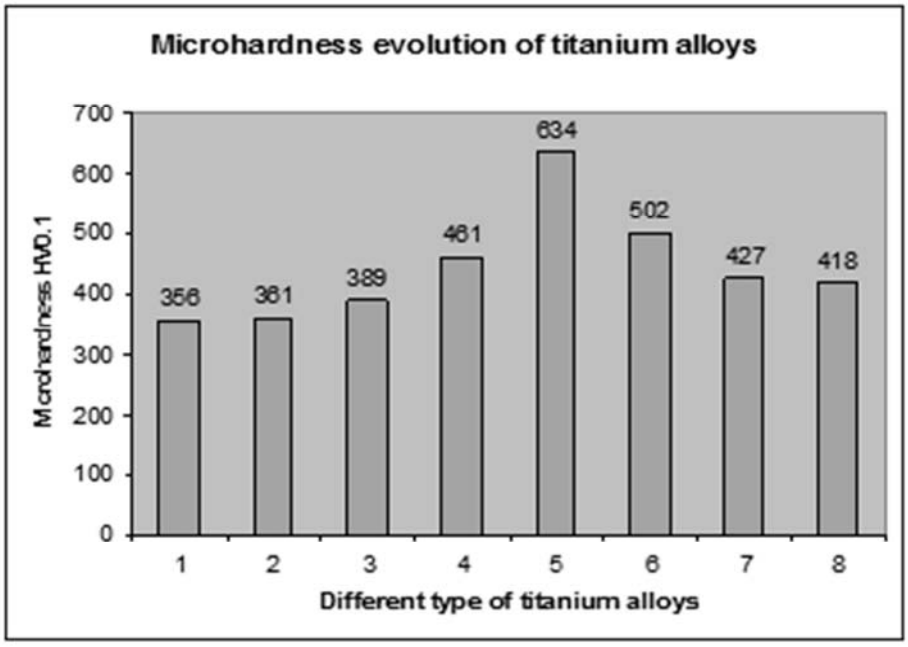

Figure 12. *The microhardness average values for different type of titanium alloys: 1 - Ti8Al4V trade mark alloy; 2 - Ti8Al4V remelted; 3- Ti8Al; 4- Ti8Al2.8Fe; 5- Ti9Al5Fe; 6- Ti5Fe; 7- Ti5.7Mn; 8- Ti3Mn*
Slika 12. *Srednje vrednosti mikrotvrdoće za različite legure titana: 1 - Ti8Al4V komercijalna oznaka legure; 2 - Ti8Al4V pretopljena; 3- Ti8Al; 4- Ti8Al2.8Fe; 5- Ti9Al5Fe; 6- Ti5Fe; 7- Ti5.7Mn; 8- Ti3Mn*

The highest value of hardness was recorded for the Ti9Al5Fe alloy (634HV0.1), benefiting from the presence of aluminium and iron, which causes the formation of hard secondary phases. Significant hardness values were also measured for Ti8Al2.8Fe (502HV0.1) and Ti5Fe (461HV0.1) alloys.

4. Conclusion

Alloying elements introduced in titanium alloy have different effects on the microstructure, the relative density and the microhardness.

Aluminium stabilizes the alpha phase in titanium alloy, having the lamellar appearance, for the content of below 8 wt% Al. Above this value, the precipitation of the compound Ti3Al appears in the form of scattered islands of irregular shape.

Iron forms three types of compounds, the most stable being TiFe2. The presence of iron increases the relative density of the alloy.

The addition of Mn in titanium reduces the alpha to beta transformation temperature and increase the relative density. Also, the presence of Mn in the titanium increases the proportion of intermetallic compound separately in the metallic matrix with finely lamellar appearance. The chemical elements that substantially increases the microhardness of titanium alloy are Fe and Al, if these are introduced simultaneously (634 HV0.1 for Ti8Al5Fe) or singular (502 HV0.1 for Ti5Fe). Effect of Mn on the increasing of hardness is less important, yielding a slight increase of microhardness from 418HV0.1 for Ti3Mn to 427HV0.1 for Ti5.7Mn. The welding behaviour of the new titanium alloys using TIG process is appropriate if the requirements for a good protection with inert gas both on the surface of the samples and at the root of the weld is respected. A more pronounced tendency of welding pore formation was recorded for Ti5Fe alloy.

By keeping low values of linear welding energy, the tendency of grain size increasing in the weld and the heat affected zone can be avoided.

Rapid cooling after welding of biocompatible titanium alloys with Mn leads to the emergence of acicular phases without the excessive increase in hardness, which is a beneficial effect in maintaining the mechanical characteristics close to those of the human bone.

Acknowledgements: This work was supported by a grant of the Romanian Ministry of Research and Innovation, CCCDI – UEFISCDI, project number PN-III-P1-1.2-PCCDI-2017-0239/60 PCCDI 2018, “OBTAINING AND EXPERTISE OF NEW BIOCOMPATIBLE MATERIALS FOR MEDICAL APPLICATIONS - MedicalMetMat”, within PNCDI III.

Najveća vrednost tvrdoće zabeležena je za leguru Ti9Al5Fe (634HV0.1), koja ima koristi od prisustva aluminijuma i gvožđa, što izaziva stvaranje čvrstih sekundarnih faza. Značajne vrednosti tvrdoće su takođe merene kod legure Ti8Al2.8Fe (502HV0.1) i Ti5Fe (461HV0.1).

4. Zaključak

Legirani elementi uvedeni u leguru titana imaju različite efekte na mikrostrukturu, relativnu gustinu i mikrotvrdoću.

Aluminijum stabilizuje alfa fazu u legurama titana, koji ima oblik lamele, za sadržaj ispod 8 tež.% Al. Iznad ove vrednosti talog jedinjenja Ti3Al se pojavljuje u obliku raštrkanih ostrva nepravilnog oblika.

Gvožđe formira tri vrste jedinjenja, od kojih je najstabilnija TiFe2. Prisustvo gvožđa povećava relativnu gustinu legure.

Dodavanje Mn u titanu smanjuje temperaturu transformacije alfa u beta i povećava relativnu gustinu. Takođe, prisustvo Mn u titanu povećava udeo intermetalnog jedinjenja odvojenog u metalnoj matrici sa fino lamelarnim izgledom.

Hemijski elementi koji značajno povećavaju mikrotvrdoću legura titana su Fe i Al, ako se uvode istovremeno (634 HV0.1 za Ti8Al5Fe) ili pojedinačno (502 HV0.1 za Ti5Fe). Uticaj Mn na povećanje tvrdoće je manje važan, što dovodi do neznatnog povećanja mikrotvrdoće sa 418HV0.1 za Ti3Mn na 427HV0.1 za Ti5.7Mn.

Ponašanje pri zavarivanju novih legura titana TIG postupkom je pogodno ako se poštuju zahtevi za dobrom zaštitom inertnim gasom i na površini uzoraka i na korenu zavara.

Zabeležena je izraženija tendencija stvaranja pora pri zavarivanju legure Ti5Fe.

Zadržavanjem niskih vrednosti linearne energije zavarivanja može se izbeći tendencija povećanja veličine zrna u šavu i zoni uticaja toplote.

Brzo hlađenje nakon zavarivanja biokompatibilnih legura titana sa Mn dovodi do stvaranja acikularnih faza bez prekomernog povećanja tvrdoće, što povoljno utiče na održavanje mehaničkih karakteristika bliskih onima ljudske kosti.

Zahvalnice: Ovaj rad je podržan grantom rumunskog Ministarstva za istraživanje i inovacije, CCCDI - UEFISCDI, broj projekta PN-III-P1-1.2-PCCDI-2017-0239 / 60 PCCDI 2018, „DOBIVANJE I EKSPERTIZA NOVIH BIOCOMPATIVNIH MATERIJALA ZA MEDICINSKE PRIMENE - MedicalMetMat ”, u okviru PNCDI III.

References
Reference

[1] M. Niinomi, Recent research and development in titanium alloys for biomedical applications and healthcare goods, Science and Technology of Advanced Materials 4 (2003) 445-454.

[2] C. Oldani, A. Dominguez, Titanium as a Biomaterial for Implants, Recent Advanced in Arthroplasty, (2012) 149-162.

[3] E.A. Levashov, M.I.Petrzhik, D.V. Shtansky, Ph.V. Kirykhantsev-Korneev, A.N. Sheveyko, R.Z. Valiev, D.V. Gunderov, S.D. Prokoshkin, A.V. Korotitskiy, A.yu. Smolin, Nanostructured titanium alloys and multicomponent bioactive films: Mechanical behaviour at indentation, Materials Science and Engineering A 570 (2013) 51-62.

[4] H. Michelle Grandin, S. Berner, M. Dard, A Review of Titanium Zirconium (TiZr) Alloys for Use in Endosseous Dental Implant, Materials 2012, Vol.5, 1348-1360.

[5] C.N. Elias, J.H.C. Lima, R.Valiev, M.A. Meyers, Biomedical Applications of Titanium and its alloys, Biological Materials Science, JOM (2008) 47-49.

[6] M. Niinomi, Biologically and Mechanically Biocompatible Titanium Alloys, Materials Transactions, Vol. 49, No 10 (2008) 2170-2178.

[7] H.W. Jeong, S.E. Kim, Y.T. Hyun, Y.T. Lee, J.K. Park, Microstructures and Elastic Moduli of Binary Titanium Alloys Containing Biocompatible Alloying Elements, Materials Science Forum, Vols. 475-479 (2005) 2291-2294.

[8] H.J. Breme, J.A. Helsen, *Metals as Biomaterials-Selection of Materials*, Biomaterials Science and Engineering Series, Wiley, (1998) 20-21.

[9] J. Malek, F. Hnilica, J. Vesely, Beta Titanium Alloy Ti35Nb6Ta with Boron Addition, *Metal 2012*, Brno, Czech Republic, p. 6.

[10] I. Ohnuma, Y. Fujita, H. Mitsui, K. Ishikawa, R. Kainuma, K. Ishida, Phase equilibrium in the Ti-Al binary system, Acta Mater. Vol. 48, Iss. 12 (2000) 3113-3123.

[11] Y.L.Hao, D.S. Xu, Y.Y. Cui, R. Yang, D.Li, Acta mater. 47 (1999) 1129.

[12] C.R. de Farias Azevedo, H.M. Flower, Microstructure and phase relationships in Ti-Al-Si System, Materials Science and Technology, Vol. 15 (1999) 869-877.

[13] N. Saunders, Phase Equilibria in Multi-Component γ-TiAl Based Alloys, “Gamma Titanium Aluminides” (1999), p. 183.

[14] F. Zhang, E. Burkel, Novel Titanium Manganese Alloys and Their Macroporous Foams for Biomedical Applications Prepared by Field assisted Sintering, Biomedical engineering, Trends in materials Science, (2011) 203-224.

[15] H.J. Breme, V.Biehl, J.A. Helsen, Metals and implants, Biomaterials Science and Engineering Series, Wiley (1998) 54-55.

[16] H.F. Hildebrand, J.C. Hornez, Biological response and biocompatibility, Biomaterials Science and Engineering Series, Wiley (1998) 268-270.

[17] F. Shank, Structure of binary alloys, Metallurgy (1973) p. 759.

[18] M. Hansen, K. Anderko, Structure of binary alloys, vol. 1 (1962) p. 607.

[19] Hansen, M., Anderko, K., Structure of binary alloys, vol. 2 (1962) p. 1487.

[20] M. Ikeda, M. Ueda, R. Matsunaga, M. Ogawa, M. Niinomi, Isothermal Aging Behaviour of Beta Titanium – manganese Alloys, Materials Transactions, Vol. 50, no.12 (2009) 2737 -2743.

[21] R. Baloyi, Investigation into the Effect of Solid Solution Chemistry on Lattice Parameters and Microstructural Properties of beta-Ti Alloys, dissertation Johannesburg, 2010.

[22] S. Tamirisakandala, R.B. Bhat, J.S. Tiley, D.B. Miracle, Grain refinement of cast titanium alloys via trace boron addition, Scripta Materialia, Vol. 53 (2005), 1421-1426.

[23] M.J. Bermingham, S.D. McDonald, M.S. Dargusch, D.H. StJohn, Microstructure of Cast Titanium Alloys, Materials Forum, volume 31 (2007) 84 – 89.

[24] Zhang F., Weidmann A., Nebe J.B., Beck U., Burkel E., Preparation, microstructures, mechanical properties and cytocompatibility of TiMn alloys for biomedical applications, J. Biomed Mater, Res B, App. Biomater, (2010), 94 (2) 406-13.

[25] I.Voiculescu, V.Geanta, E.M. Binchiciu, P. Vizureanu, H. Binchiciu. Welding behaviour of new biocompatible titanium alloys. VIIIth International Metallurgical Congress, Ohrid, Macedonia, 2018.

[26] I. Voiculescu, O.G. Donţu, V. Geantă, S. Ganatsios, Effect of the Laser Beam Superficial Heat Treatment on the Gas Tungsten Arc Ti-6Al-V Welded Metal Microstructure, Conference on Industrial Laser Applications (INDLAS 2007) Bran, ROMANIA , INDUSTRIAL LASER APPLICATIONS, Proceedings of SPIE, Vol. 7007, Article no.: 70070M (2007).

R. Kshirsagar [1,a], S. Jones [2,b], J. Lawrence [1,c], J. Tabor [3,d]

Introduction of a New Term - Ferrite Number Density (FND) to Measure the Ferrite Number of Welds on Thin 300 Series Stainless Steel Sheets

Uvođenje novog termina – Gustina feritnog broja (FND) za merenje feritnog broja zavarenih spojeva na tankim limovima od nerđajućeg čelika serije 300

Originalni naučni rad / Original scientific paper
Rad je u izvornom obliku objavljen u okviru 71. IIW godišnje Skupštine i međunarodne konferencije održane na Baliju-Indonezija 15-20. Jula 2018
Rad primljen / Paper received:
Oktobar 2019.

Ključne reči: Feritni broj, zavarivanje tankih limova, Gustina feritnog broja, FeritScope®, FGAB1.3-Fe sonda, odnos gledišta

Adresa autora / Author's address:
[1] *Institute for Advanced Manufacturing and Engineering, Convetry University, Coventry, UK*
[2] *Nuclear Advanced Manufacturing Research Centre, University of Sheffield, Sheffield, UK*
[3] *sigma Maths and Stats Support Centre, Convetry University, Coventry, UK*
[a] *kshirsar@uni.coventry.ac.uk,* [b] *steve.jones@namrc.co.uk,* [c] *ac5588@coventry.ac.uk,* [d] *mtx041@coventry.ac.uk*

Key words: Ferrite Number, welding of thin sheets, Ferrite Number Density, FeritScope®, FGAB1.3-Fe probe, aspect ratio

Abstract

Delta-ferrite content in austenitic steel welds is a crucial parameter to control, since a number of properties depend on this. A FeritScope® is commonly used commercially to measure the Ferrite Number (FN) of the welds which takes advantage of the fact that the retained delta-ferrite phase at room temperature is magnetic whereas austenite is not. However, the readings obtained from the FeritScope® are influenced by a number of constraints such as sheet thickness, weld clad thickness, etc. Although some correction factors have been introduced by the FeritScope® manufacturer to account for these influential conditions, some other geometrical features of the welds were also found to influence the measured FN; for example, despite being a major influential parameter, there is no factor introduced to correct the measurement inconsistencies associated with smaller weld crown widths. In addition, the results obtained on measuring the FN using a FeritScope® contradicted the trends that were expected considering the literature. This research introduces a term called Ferrite Number Density (FND) to represent the ferrite content, in which the measured FN is further proportioned with the cross-sectional area of the weld bead, thus eliminating its dependency on the geometrical size of the weld. It has been established from this research that for welds completed on sheets thicker than 2.4 mm, the FN can be directly used as an indicator of the ferrite content in the weld; however, for thinner sheets, the FND must be used to indicate the ferrite

Rezime

Sadržaj delta-ferita u zavarenim spojevima od austenitnih čelika je presudni parametar za kontrolu, jer od toga zavisi niz svojstava. FeritScope® se obično komercijalno koristi za merenje feritnog broja (FN) zavarenih delova koji koristi činjenicu da je zaostala delta-feritna faza na sobnoj temperaturi magnetna, dok austenit nije. Međutim, očitavanja dobijena FeritScope®-om utiče niz ograničenja kao što su debljina lima, debljina plakature i sl. Iako je proizvođač FeritScope® uveo neke faktore korekcije da bi objasnio ove uticajne uslove, neke druge geometrijske karakteristike zavarenih spojeva takođe utiču na izmereni FN; na primer, uprkos tome što je glavni uticajni parametar, nije uveden faktor koji bi ispravio neusklađenosti merenja povezanih sa manjim širinama vrhova zavarenih spojeva. Pored toga, rezultati dobijeni merenjem FN-a upotrebom FeritScope®-a bili su u suprotnosti sa trendovima koji su bili očekivani uzimajući u obzir literaturu. Ovo istraživanje uvodi termin nazvan Gustina Feritnog broja (FND) da bi predstavio sadržaj ferita, u kome je izmereni FN dodatno proporcionalan sa površinom poprečnog preseka zavara, čime se eliminira njegova zavisnost od geometrijske veličine zavara. Iz ovog istraživanja utvrđeno je da se za zavare izrađene na limovima debljim od 2,4 mm, FN može direktno koristiti kao pokazatelj sadržaja ferita u šavu; međutim, za tanje limove FND se mora koristiti za označavanje sadržaja ferita u zavarivanju, ako se upotrebljava FeritScope® sa sondom odmerene veličine, npr. u ovom slučaju

content of the weld, if a FeritScope® with an apportioned size probe is used, e.g. in this case an FGAB1.3-Fe probe. Use of FND eliminated all the contradictions obtained between experimental data and literature for thin sheet welds.

1. Introduction

Generally, austenitic stainless steel welds are expected to have a dual-phase microstructure to eliminate deleterious imperfections from forming within the weld microstructure in austenite-to-ferrite proportions ranging between 95/5 to 90/10 respectively. The amount of retained delta-ferrite in the weld depends mainly on the chemical composition of the materials being joined [1], filler material (if used) and the cooling rate of the weld pool [2]. The amount of retained delta-ferrite in the welds is measured using a Ferrite Number (FN) scale, which has been defined in various internationally accepted standards such as ISO 8249 and AWS A4.2M. In austenitic stainless steels, the presence of small amounts of ferrite is known to have beneficial effects on the weld properties [3]. One of the most significant benefits of retaining these small amounts of delta-ferrite during solidification is that it increases the weld's resistance to solidification cracking, especially in presence of sulphur and phosphorous impurities [4]. However, having larger quantities of delta ferrite (>10 FN) can lead to the formation of the brittle sigma phase within the weld on exposure to high temperatures (425°C to 550°C) for extended times. This influence of delta-ferrite on weldments makes it necessary to measure the ferrite content of austenitic stainless steel welds. Various methods and instruments have been developed in order to measure either the ferrite content (in percentage) or the FN of austenitic steel welds, either destructively or non-destructively. The destructive tests include image analysis of etched metallographic specimen, electrochemical examination [5], etc. The non-destructive methods take advantage of the fact that delta-ferrite at room temperature is magnetic, in a non-magnetic austenite matrix. Although a number of instruments are commercially available for measuring the FN of the welds, one of the most commonly used is a FeritScope®, developed by Fischer Scientific. The FeritScope® measures the FN using a magnetic induction method, consequently measuring all the magnetic phases within the weld including the delta-ferrite as well as any strain-induced martensite that may have formed during large deformation processes. Most of the alloying elements present in austenitic stainless steel can be classified into austenite- promoting and ferrite-promoting elements [6]. The

sonda FGAB1.3-Fe. Upotrebom FND-a otklonjene su sve kontradikcije dobijene između eksperimentalnih podataka i literature za zavarene tanke limove.

1. Uvod

Uopšteno, očekuje se da će austenitni zavareni spojevi imati dvofaznu mikrostrukturu radi eliminisanja nastajanja štetnih nesavršenosti unutar mikrostrukture šava, u proporcijama austenit-ferit između 95/5 do 90/10. Količina zaostalog delta-ferita u šavu uglavnom zavisi od hemijskog sastava osnovnih materijala [1], dodatnih materijala (ako se koristi) i brzine hlađenja zavarivačke kupke [2]. Količina zaostalog delta-ferita u šavovima se meri korišćenjem skale feritnog broja (FN), koja je definisana u raznim međunarodno prihvaćenim standardima, kao što su ISO 8249 i AWS A4.2M. Poznato je da prisustvo malih količina ferita u austenitnim nerđajućim čelicima ima blagotvoran uticaj na svojstva šava [3]. Jedna od najznačajnijih prednosti zadržavanja tih malih količina delta-ferita tokom očvršćavanja je ta što povećava otpornost šava solidifikacione prsline, posebno u prisustvu nečistoća sumpora i fosfora [4]. Međutim, veće količine delta ferita (> 10 FN) mogu dovesti do stvaranja krte sigma faze unutar šava izloženog visokim temperaturama (425 ° C do 550 ° C) tokom dužeg vremena. Ovaj uticaj delta-ferita na zavarene spojeve čini neophodnim merenje sadržaja ferita u zavarenim spojevima od austenitnih nehrđajućih čelika.

Razvijene su različite metode i instrumenti za merenje sadržaja ferita (u procentima) ili FN austenitnih zavarenih spojeva, bilo sa ili bez razaranja. Ispitivanja sa razaranjem uključuju analizu slike nagriženog metalografskog uzorka, elektrohemijsko ispitivanje [5] itd. Kod metoda bez razaranja, koristi se činjenica da je delta-ferit na sobnoj temperaturi magnetičan, u nemagnetničnoj austenitnoj matrici. Iako je komercijalno dostupan veliki broj instrumenata za merenje FN zavarenih spojeva, jedan od najčešće korišćenih je FeritScope®, koji je razvio Fischer Scientific. FeritScope® meri FN metodom magnetne indukcije, mereći sve magnetne faze u šavu, uključujući delta-ferit, kao i martenzit izazvan deformacijom koji se može formirati tokom procesa velikih deformacije.

Većina legirajućih elemenata prisutnih u austenitnom nerđajućem čeliku može se svrstati u elemente koji promovišu austenit i ferit [6]. Elementi koji promovišu austenit, kao što su nikl (Ni), ugljenik (C), azot (N) i bakar (Cu), ubrzavaju stvaranje austenita u zavarivačkoj kupki tokom očvršćavanja.

austenite-promoting elements such as nickel (Ni), carbon (C), nitrogen (N) and copper (Cu) accelerate the formation of austenite in the weld pool during solidification. They have been collectively quantified as nickel equivalent (Nieq) in the WRC-1992 Ferrite Number prediction diagram. Likewise, the ferrite promoting-elements, that include chromium (Cr), molybdenum (Mo) and niobium (Nb), have been collectively termed as chromium equivalent (Creq). It has been reported by [6] while developing the WRC-1992 diagrams that the relative quantities of Creq and Nieq determine the amount of delta-ferrite that will be retained in the solidified weld when the arc welding process is used. As mentioned earlier, apart from the chemical composition, the weld pool cooling rate is also believed to significantly affect the amount of delta ferrite retained. A number of researchers have reported a shift in solidification mode from primary ferrite to primary austenite at extremely high cooling rates, such as in case of laser [7] and electron beam welding [8]. Still, at low to moderate cooling rates, typically obtained in TIG welding, the weld pool is expected to solidify primarily as ferrite (depending on the chemistry of the materials), known as FA type of solidification [6]. In this type of solidification mode, the amount of retained delta-ferrite increases with an increase in the cooling rate. This is because at high cooling rates, the diffusion controlled ferrite to austenite transformation is supressed owing to insufficient time. In the present research, the influence of weld bead geometry on measured FNs using a FeritScope® for thin sheets (< 2.4 mm) has been investigated. The measured FNs show results contradicting those reported in literature such as the effect of cooling rate on the retained delta-ferrite. It is believed that in addition to the influential parameters mentioned in the FeritScope® user manual [9], the weld bead width and consequently the weld cross-sectional area can have a significant effect on the measured FNs. A new term, Ferrite Number Density (FND) has been introduced, which can be a better indicator of the ferrite content in a solidified weld by eliminating the influence of these geometrical features, especially in thin sheet joints. Using the FND instead of FN also eliminated the contradictions obtained when experimental results were compared to the literature.

2. Methodology

2.1 Experimental Procedure

A number of 304L stainless steel sheets having various thicknesses were welded using an automated tungsten inert gas (TIG) welding process. The sheet thicknesses used for the

Oni su zajednički kvantifikovani kao ekvivalent nikla (Ni_{ek}) u dijagramu predviđanja feritnog broja WRC-1992. Isto tako, feritni promotivni elementi, koji uključuju hrom (Cr), molibden (Mo) i niobijum (Nb), zajedno su nazvani hromovim ekvivalentom (Cr_{ek}). Saopšteno je [6] tokom izrade dijagrama WRC-1992. da relativne količine Cr_{ek}-a i Ni_{ek}-a određuju količinu delta-ferita koja će se zadržati u očvrslom šavu pri elektrolučnim postupcima zavarivanja. Kao što je ranije spomenuto, osim hemijskog sastava, veruje se da i brzina hlađenja kupke značajno utiče na količinu zaostalog delta ferita.

Brojni istraživači su izvestili da je prelazak u režimu očvršćavanja sa primarnog ferita na primarni austenit, pri ekstremno visokim brzinama hlađenja, kao što je slučaj u slučaju laserskog [7] i zavarivanja elektronskim snopom [8]. Ipak, pri niskim do umerenim brzinama hlađenja, koje se obično dobijaju pri TIG zavarivanju, očekuje se da kupka očvrsne prevashodno kao ferit (zavisno od hemije materijala), poznat kao FA vrsta očvršćivanja [6]. U ovom načinu očvršćavanja, količina zaostalog delta-ferita raste sa porastom brzine hlađenja. To je zato što se pri visokim brzinama hlađenja difuziona transformacija ferita do austenita potiskuje zbog nedovoljnog vremena.

U ovom istraživanju je istražen uticaj geometrije zavara na izmerene FN-ove pomoću FeritScope®-a za tanke limove (<2,4 mm). Izmereni FN pokazuju rezultate suprotne onima koji su navedeni u literaturi, kao što je efekat brzine hlađenja na zaostali delta-ferit. Veruje se da pored uticajnih parametara navedenih u korisničkom priručniku FeritScope® [9], širina zavara i posledično područje poprečnog preseka šava mogu imati značajan uticaj na izmerene FN. Uveden je novi termin Gustina feritnog broja (FND), koji može biti bolji pokazatelj sadržaja ferita u očvrslom šavu, eliminišući uticaj ovih geometrijskih karakteristika, naročito na spojevima tankih ploča. Korišćenjem FND-a umesto FN-a takođe su eliminisane kontradikcije dobijene prilikom upoređivanja eksperimentalnih rezultata sa literaturom.

2. Metodologija

2.1 Postupak eksperimenta

Brojni limovi od nerđajućeg čelika 304L raznih debljina zavareni su automatskim TIG postupkom zavarivanja. Debljina lima korišćena za eksperimente bila je 0,7 mm, 0,9 mm, 1,5 mm, 2,0

experiments were 0.7 mm, 0.9 mm, 1.5 mm, 2.0 mm and 2.4 mm. The chemical composition of all these sheet materials is mentioned in Table 1. Sheets thinner than 1.5 mm were welded autogenously i.e. without any filler material. This ensured that the weld pool chemistry remained unaltered, except in the cases where nitrogen gas was deliberately added to the weld pool through the shielding gas, which has been explained later in this section. Sheets thicker than and including 1.5 mm were welded using a 308LSi filler wire, the chemistry for which is also mentioned in Table 1. The parameter ranges for every thickness were established from trial experiments that give full penetration of the joint in most cases. High purity argon (99.995%) was used as a shielding gas, however, for some experiments nitrogen gas was added to the shielding gas in order to validate the results and modify the phase distribution in the weld pool, as N2 is known to be a strong austenite promoting element. The gas compositions used for these experiments utilised 2.5% or 5% or 10% nitrogen in argon. Irrespective of shielding gas composition, high purity argon was used as the backing gas for all the experiments. The shielding gas flow rate was maintained at 8 l/min, whereas the backing gas flow rate was maintained at 5 l/min. The arc length was kept constant at 2.5 mm, which ensured that the arc voltage and the power density remained constant for a particular welding atmosphere. All experiments were done using a pulsed current waveform. Consequently, for the autogeneous welds, peak welding current (Ip), torch travel speed (S), duty cycle (δ) and the nitrogen content (N2) in the shielding gas could be varied between experiments in order to cover a wide range of heat inputs and the cooling rates of the weld pool. For the sheets that were heterogeneously welded (welded using filler materials), among the parameters mentioned above, the duty cycle was kept constant at 50%, but the filler wire feed rate (R) and the filler wire diameter (D) could be varied in order to alter the chemical composition of the weld pool. In addition to this, the pulsing frequency (f) was also varied between experiments, although it has no direct influence on the heat input to the weld pool. The minimum and maximum values of the parameters used in case of autogeneous and heterogeneous welds are mentioned in Table 2 and Table 3 respectively.

In order to develop a suitable design of experiment, among all the parameters mentioned above, Ip, S, δ, f and R were considered as continuous parameters. Due to the limitation on the materials

mm i 2,4 mm. Hemijski sastav svih ovih limova naveden je u Tabeli 1. Limovi tanji od 1,5 mm su zavareni autogeno, tj. bez ikakvog dodatnog materijala. Ovo je osiguralo da hemija zavarivačke kupke ostaje nepromenjena, osim u slučajevima kada je gas azot namerno dodat u kupku kroz zaštitni gas, što je objašnjeno kasnije u ovom odeljku. Limovi deblji od i uključujući 1,5 mm zavareni su dodatnim materijalom žicom 308LSi, čija hemija je takođe navedena u Tabeli 1. Parametri opsega za svaku debljinu su utvrđeni iz eksperimentalnih pokušaja koji u većini slučajeva daju potpuno uvarivanje spoja. Argon visoke čistoće (99,995%) korišćen je kao zaštitni gas, međutim, za neke eksperimente, dodat je azot u zaštitni gas da bi se potvrdili rezultati i modifikovala fazna raspodela u zavarivačkoj kupki, jer je poznato da je N_2 snažan element za promociju austenita. Sastavi gasnih mešavina korišćenih za ove eksperimente su sa 2,5% ili 5% ili 10% azota u argonu. Bez obzira na sastav zaštitnog gasa, argon visoke čistoće korišćen je kao osnovni za sve eksperimente. Brzina protoka zaštitnog gasa je održavana na 8 l/min, dok je protok povratnog gasa održavan na 5 l min. Dužina luka je održavana konstantnom na 2,5 mm, što osigurava da napon luka i gustina struje ostaju konstantni za određenu atmosferu zavarivanja. Svi eksperimenti su rađeni korišćenjem talasnog pulsnog oblika struje. Shodno tome, za autogene zavare, vršna struja zavarivanja (Ip), brzina kretanja gorionika (S), radni ciklus (d) i sadržaj azota (N_2) u zaštitnom gasu mogu se menjati između eksperimenata kako bi se pokrivao širok raspon unosa toplote i brzine hlađenja kupke. Za limove koji su heterogeno zavareni (zavareni upotrebom dodatnog materijala), među gore pomenutim parametrima, radni ciklus je bio konstantan na 50%, ali brzina dodatnog materijala žice (R) i prečnik žice (D) mogu se menjati u cilju izmene hemijskog sastava zavarivačke kupke. Pored toga, frekvencija pulsiranja (f) takođe je varirala između eksperimenata, mada nema direktan uticaj na dovod toplote u zavarivačku kupku. Minimalne i maksimalne vrednosti parametara koji se koriste u slučaju autogenih i heterogenih zavarivanja navedeni su u tabeli 2 i tabeli 3.

Da bi se razvio odgovarajući dizajn eksperimenta, među svim gore pomenutim parametrima, Ip, S, d, f i R su razmatrani kao kontinuirani parametri. Zbog ograničenja raspoloživih materijala i opreme, D i N_2 su smatrani diskretnim parametrima. S obzirom na mogućnost nelinearne zavisnosti zaostalog delta-ferita od parametara zavarivanja, korišćen je konvencionalni centralni kompozitni dizajn (CCD)

and equipment available, D and N2 were considered as discrete parameters. Considering the possibility of a non-linear dependence of retained delta-ferrite on the welding parameters, a conventional central composite design (CCD) of experiments scheme was used. Consequently, for every combination of discrete parameters, with four continuous parameters, 31 experiments were required at each thickness. In order to reduce the total number of experiments, only some of these were repeated for other combinations of the discrete parameters. For example, for a 0.7 mm thick sheet, 31 experiments using the CCD scheme were performed using pure argon, from which only 17 random experiments were repeated for every level of nitrogen concentration (2.5%, 5% and 10%) in the shielding gas. Consequently, nearly 85 experiments were performed at every thickness, for all of which, the Ferrite Number, bead geometry and the cross-sectional area was measured as explained in the following sections.

eksperimentalne šeme. Shodno tome, za svaku kombinaciju diskretnih parametara, sa četiri kontinuirana parametra, potreban je 31 eksperiment u svakoj debljini. Da bi se smanjio ukupan broj eksperimenata, samo su neki od njih ponovljeni za druge kombinacije diskretnih parametara. Na primer, za lim debljine 0,7 mm izvedeno je 31 eksperimenta po CCD shemi pomoću čistog argona, iz kojih je ponovljeno samo 17 nasumičnih eksperimenata za svaki nivo koncentracije azota (2,5%, 5% i 10%) u zaštitnom gasu . Shodno tome, izvedeno je gotovo 85 eksperimenata u svakoj debljini, za koji je meren feritni broj, geometrija zavara i površina poprečnog preseka kao što je objašnjeno u sledećim odeljcima.

Thickness (mm)	C	Cr	Mn	N	Ni	P	S	Si
0.7	0.019	18.290	1.130	0.064	8.250	0.035	0.001	0.310
0.9	0.023	18.140	1.750	0.090	8.180	0.041	0.003	0.200
1.5	0.026	17.795	2.000	0.100	8.120	0.025	0.001	0.497
2.0	0.015	17.685	1.669	0.071	8.075	0.033	0.001	0.320
2.4	0.0186	18.200	1.434	0.0378	8.050	0.0306	0.0037	0.401
Filler 308LSi	0.010	20.000	1.800	0.000	10.000	0.015	0.015	0.800

Table 1. *Chemical Composition of materials used for the experiments*
Tabela 1. *Hemijski sastav materijala korišćenih u eksperimentima*

2.2 Ferrite Number Measurement

A Fischer FeritScope® FMP30 with an FGAB1.3-Fe probe was used to measure the FNs of the welds obtained from the experiments. The FN for every weld was taken as an average of 10 readings at different locations along the length of weld. Since the sheets used for the experiments were thin, the measured FNs were required to be multiplied by a correction factor corresponding to that particular thickness and measured FN, the guidelines for which have been mentioned in the user manual [9] of the FeritScope®. However, in the manual, the correction factor curves are plotted only for a few discrete values of FNs, from which others required values being obtained through interpolation. The true FNs were obtained from the measured FNs using Equation (1).

$$(FN)_{ture}=(FN)_{observed}*Correction\ Factor \quad (1)$$

2.2 Merenje feritnog broja

Fischer FeritScope® FMP30 sa FGAB1.3-Fe sondom korišćen je za merenje FN-a šavova dobijenih eksperimentima. FN za svaki šav uzet je u proseku 10 očitavanja na različitim lokacijama duž dužine šava. Pošto su limovi korišćeni za eksperimente tanki, trebalo je da se mereni FN umnože korekcijskim faktorom koji odgovara toj određenoj debljini i izmerenom FN, prema smernicama koje su pomenute u korisničkom priručniku [9] FeritScope®. Međutim, u priručniku su krive korekcijskog faktora prikazane samo za nekoliko diskretnih vrednosti FN-a od kojih se interpolacijom dobijaju druge potrebne vrednosti. Pravi FN su dobijeni iz izmerenih FN pomoću jednačine (1).

$$(FN)_{ture}=(FN)_{observed}*Correction\ Factor \quad (1)$$

Figure 1 shows the difference between the true and measured FNs when the correction factors were applied to some of the readings obtained from those 0.7 mm thick sheet welds as an example. It can be clearly seen that the true FNs are considerably higher than the measured FNs. In all the subsequent sections in this paper, the term FN refers to the true FNs and not the measured values. Similarly, the correction factors for the curvature of the specimen being measured have also been mentioned in the user manual of the FeritScope®. This correction factor is required only if the radius of curvature of the specimen for which the FN is measured is less than 50 mm. Consequently, for the welds done heterogeneously, this correction factor was taken into account along with the correction factor for the thickness, depending on the radius of the crown determined from macrographic examination.

Metallographic samples were taken from all the welds in order to measure their cross-sectional area. These samples were etched using the acetic-glycergia (5 ml glycerol, 15 ml hydrochloric acid, 10 ml nitric acid and 10 ml acetic acid) solution, in order to be able to distinctly see the delta-ferrite dendrites within the austenite grains in the microstructure. A Leica DM2700 microscope was used to capture the images of the weld microstructure. The ferrite content of the welds was also quantified by applying the image analysis technique on the microstructural images obtained. ImageJ software was used to measure the ferrite content, which has been detailed in the later sections.

2.3 Heat Input and Cooling Rate Calculations

For all the welds, the heat input and the cooling rate of the weld was calculated using the analytical expressions derived by [10]. This was done in order to understand the effect of cooling rate on the residual delta-ferrite content. However, the results obtained contradicted the trends available in the literature, which led to the belief that some other factors, apart from the ones mentioned in the FeritScope® user manual must be influencing the measured FNs.

2.3.1 Heat Input Calculations

In general, for an arc welding process using a pulsed waveform, the heat input to the weld pool is a function of effective welding current, the torch travel speed and the voltage across the arc (which is defined by the arc length and the welding atmosphere). The heat input, neglecting thermal efficiency (η) is expressed in J/mm and is calculated using Equation (2).

Na slici 1 prikazana je razlika između pravih i izmerenih FN-ova kada su korektivni faktori primenjeni na neke od očitavanja dobijenih iz tih zavarenih spojeva na 0,7 mm debelim limovima. Jasno se vidi da su pravi FN-ovi znatno veći od izmerenih FN-ova. U svim narednim odeljcima ovog rada, termin FN se odnosi na prave FN-ove, a ne na izmerene vrednosti.

Slično tome, korektivni faktori za zakrivljenost uzorka koji se mere su takođe navedeni u korisničkom priručniku FeritScope®. Ovaj korekcioni faktor potreban je samo ako je poluprečnik zakrivljenosti uzorka za koji se meri FN manji od 50 mm. Shodno tome, za heterogeno zavarene spojeve, uzet je u obzir i ovaj korekcioni faktor, zajedno sa korekcionim faktorom za debljinu, u zavisnosti od radijusa vrha, određenih makrografskim pregledom.

Uzeti su metalografski uzorci svih šavova kako bi se izmerila njihova površina poprečnog preseka. Ovi uzorci su nagriženi rastvorom kiselina u glicerinu (5 ml glicerina, 15 ml hlorovodonične kiseline, 10 ml azotne kiseline i 10 ml sirćetne kiseline) kako bi se mogli jasno videti delta-feritni dendriti unutar zrna austenita u mikrostrukturi. Za snimanje mikrostrukture korišćen je mikroskop Leica DM2700. Sadržaj ferita u šavovima je takođe kvantifikovan primenom tehnike analize slike na dobijenim mikrostrukturnim slikama. Softver Image J je korišćen za merenje sadržaja ferita, što je detaljno opisano u kasnijim odeljcima.

2.3 Proračun unete toplote i brzine hlađenja

Za sve šavove, unos toplote i brzina hlađenja šava izračunata je korištenjem analitičkih izraza dobijenih sa [10]. Ovo je urađeno da bi se razumeo uticaj brzine hlađenja na zaostali sadržaj delta-ferita. Međutim, dobijeni rezultati su u suprotnosti s trendovima dostupnim u literaturi, što je dovelo do uverenja da neki drugi faktori, osim onih koji se spominju u FeritScope® korisničkom priručniku, moraju uticati na izmerene FN.

2.3.1 Izračunavanje umete toplote

Uopšteno, za neki elektrolučni postupak zavarivanja uz upotrebu pulsirajućeg talasnog oblika, unos toplote u kupku je funkcija efektivne struje zavarivanja, brzine kretanja gorionika i napona duž luka (što je definisano dužinom luka i atmosferom zavarivanja). Unos toplote, zanemarujući toplotnu efikasnost (η), izražava se u J / mm i izračunava se pomoću jednačine (2).

$H=(Ie*V)/S$ (2)

where,

H is the heat input (J/mm)

V is the arc voltage (V)

S is the torch travel speed (mm/s)

I_e is the effective current (A), which in the case of a pulsed waveform is calculated using

$Ie=\sqrt{(Ip2)}*\delta + (Ib2)*(1-\delta)$ (3)

where,

Ip is the peak current,

Ib is the base current

δ is the duty cycle.

The heat source power (q) which is required to obtain the cooling rate was calculated using Equation (4).

$q=Ie*V$ (4)

The reason for neglecting the thermal efficiency (η) within this study is that the value of 0.6 applied to the TIG process in the standard EN1011 is an average and could skew comparative studies completed by any future researchers wishing to assess this work.

$H=(Ie*V)/S$ (2)

gde je,

H je unos toplote (J / mm)

V je napon luka (V)

S brzina kretanja gorionika (mm / s)

tj. Efektivna struja (A) koja se u slučaju pulsnog talasnog oblika izračunava koristeći

$Ie=\sqrt{(Ip2)}*\delta + (Ib2)*(1-\delta)$ (3)

gde je,

Ip vršna struja,

Ib osnovna struja

d radni ciklus

Snaga izvora toplote (q) koja je potrebna za postizanje brzine hlađenja izračunata je pomoću jednačine (4).

$q=Ie*V$ (4)

Razlog zanemarivanja toplotne efikasnosti (η) u okviru ove studije je taj što je vrednost 0,6, koja se primenjuje na TIG postupak u standardu EN1011, prosečna i može da iskrivi uporedne studije koje bi završili bilo koji budući istraživači koji žele da procene ovaj rad.

Sheet Thickness →	0.7 mm		0.9 mm	
Parameter	Minimum	Maximum	Minimum	Maximum
Peak Welding Current (A)	50	70	60	80
Torch Travel Speed (mm/s)	4	6	4	6
Duty Cycle (%)	40	60	40	60
Pulsing Frequency (Hz)	4	8	4	8
Nitrogen content in shielding gas (%)	0	10	0	10

Table 2. *Parameter ranges used for autogenous welds*

Tabela 2. *Opseg korišćenih parametara za autogene šavove*

Sheet Thickness →	1.5 mm		2.0 mm		2.4 mm	
Parameter	Minimum	Maximum	Minimum	Maximum	Minimum	Maximum
Peak Welding Current (A)	60	120	60	160	90	160
Torch Travel Speed (mm/s)	2	4	1	6	1	3
Pulsing Frequency (Hz)	1	6	1	10	1	6
Filler Wire Feed Rate (mm/min)	100	700	100	900	150	700
Filler Wire Diameter (mm)	0.8	1	0.8	1	0.8	1
Nitrogen content in shielding gas (%)	0	10	0	10	0	10

Table 3. *Parameter ranges used for heterogeneous welds*

Tabela 3. *Opseg korišćenih parametara za heterogene šavove*

Therefore the heat input and the heat source power was calculated for all the welds using Equation (1), (2) and (3), following which the cooling rates were obtained from the expressions shown below.

Stoga su ulazna toplota i snaga izvora toplote izračunati za sve šavove pomoću jednačine (1), (2) i (3), nakon čega su brzine hlađenja dobijene iz izraza prikazanih dole.

2.3.2 Cooling Rate Calculations

The cooling rate of the weld pool was calculated using either the 2-D or the 3-D cooling rate expression since the welds obtained were a mixture of full and partially penetrated fusion profiles. The

2.3.2 Izračunavanje brzine hlađenja

Brzina hlađenja kupke je izračunata korišćenjem ili 2-D ili 3-D izraza brzine hlađenja, jer su dobijeni šavovi bili mešavina potpuno i delimično uvarenih

expressions for 2-D and 3-D cooling rates used are shown in Equation (5) and Equation (6) respectively.

$$R_{2D} = 2\pi K\rho C_p \left(\frac{(S/10)t}{q}\right)^2 (T' - T_0)^3 \quad (5)$$

$$R_{3D} = 2\pi K \left(\frac{(S/10)}{q}\right)^2 (T' - T_0)^2 \quad (6)$$

where,
R_{2D} and R_{3D} is the 2-D and the 3-D cooling rate respectively (°C/s),
K is the thermal conductivity (W/cm-°C),
ρ is the density (g/cm3),
Cp is the specific heat (J/g-°C)
S is the torch travel speed (mm/s),
t is the thickness (cm)
q is the heat source power (watts)
T' is the temperature at which the cooling rate is calculated (°C)
T_0 is the initial plate temperature
Table 4 summarizes the values of the constant parameters used in Equations (5) and (6) for the calculation of the cooling rate of the weld. These values are the same as those used by [11] to estimate the cooling rate for the prediction of Ferrite Numbers. Whether a 2-D cooling rate

profila stpanja. Izrazi za korišćene 2-D i 3-D brzine hlađenja prikazani su u jednačini (5) i jednačini (6).

$$R_{2D} = 2\pi K\rho C_p \left(\frac{(S/10)t}{q}\right)^2 (T' - T_0)^3 \quad (5)$$

$$R_{3D} = 2\pi K \left(\frac{(S/10)}{q}\right)^2 (T' - T_0)^2 \quad (6)$$

gde je,
R_{2D} i R_{3D} su 2-D i 3-D brzina hlađenja, respektivno (° C / s),
K je toplotna provodljivost (W / cm- ° C),
r je gustina (g / cm^3),
Cp je specifična toplota (J / g- ° C)
S brzina kretanja gorionika (mm / s),
t debljina (cm)
q je snaga izvora toplote (vati)
T 'je temperatura pri kojoj se izračunava brzina hlađenja (° C)
T_0 je početna temperatura ploče
U tabela 4 sumirane su vrednosti konstantnih parametara korišćenih u jednačinama (5) i (6) za proračun brzine hlađenja šava. Ove vrednosti su iste kao i one koje koristi [11] za procenu brzine hlađenja za predviđanje feritnih brojeva. Da li se primenjuje dvosmerna brzina hlađenja

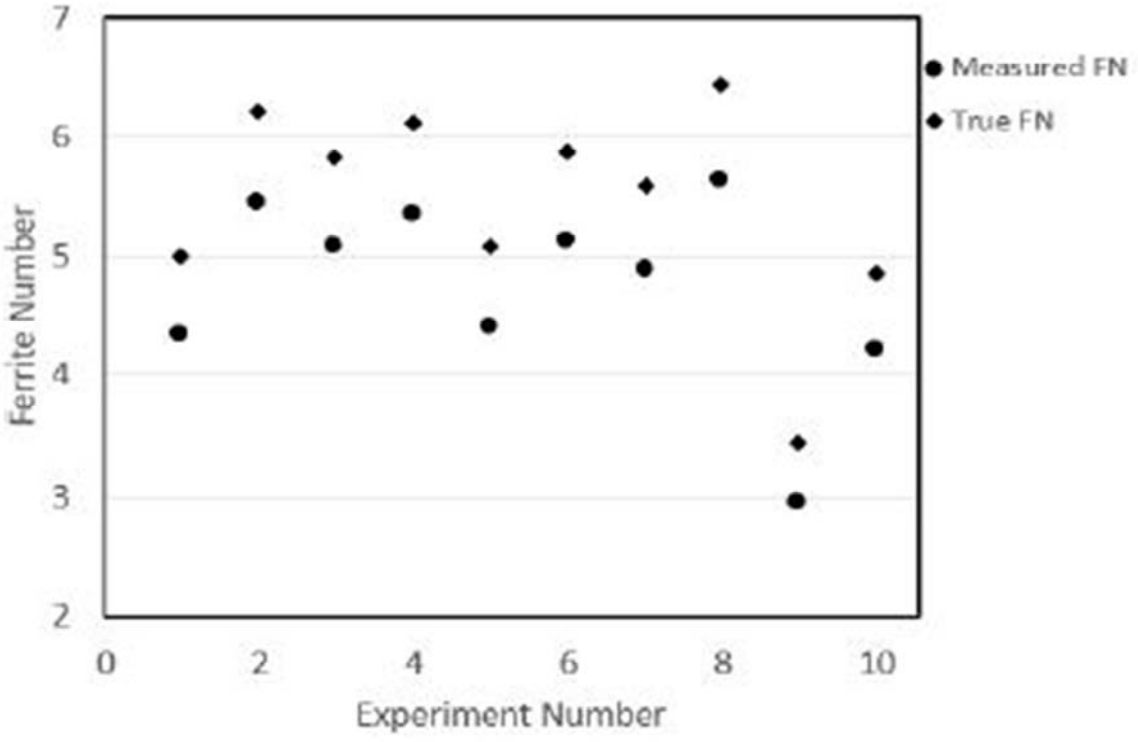

Figure 1. *Difference between True FN and measured FN for 0.7 mm thick sheet welds*
Slika 1. *Razlika između stvarnog FN i izmerenog FN za šavove od lima debljine 0,7 mm*

or a 3-D cooling rate applies depends on the relative plate thickness (τ), which can be estimated using Equation (7) as mentioned in the ASM Welding Handbook [12].

ili trosmerna brzina hlađenja zavisi od relativne debljine lima (t), koja se može proceniti pomoću jednačine (7) kao što je spomenuto u ASM priručniku za zavarivanje [12].

$$\tau = t * \sqrt{(\rho C_p V(T' - T_0)/q} \quad (7)$$

According to the Welding Handbook, if τ < 0.6, a 2-D cooling rate expression must be used, but if τ > 0.9, the 3-D cooling rate expression must be used. However, [2] found that this criteria was not optimal and modified it such that, a 2-D cooling rate expression was used when the value of τ was less than 1.5, and a 3-D cooling rate expression was used when the value of τ was greater than 2.0. For values in between these, an average of 2-D and 3-D cooling rates was considered. This cooling rate was used as one of the input parameter to predict the FN in the Oak Ridge Ferrite Number (ORFN) model. In this research, the criteria used by [2] is applied to calculate the cooling rates, since the FN values obtained from experiments could then be compared to the values predicted by the ORFN model.

3. Results and Discussion

From the results obtained, the influence of the cooling rate on the FN was studied. Figure 2 shows plots of measured FNs against the cooling rates calculated for the welded joints of various thickness sheets.

It can be seen from Figure 2 that as the cooling rate is increased, the amount of retained delta-ferrite is decreased for welds completed on the 0.7 mm, 0.9 mm, 1.5 mm and 2.0 mm thick sheets. The 2.4 mm thick sheet did not show such a trend, the possible reason for which is explained in the later sections.

$$\tau = t * \sqrt{(\rho C_p V(T' - T_0)/q} \quad (7)$$

Prema Priručniku za zavarivanje, ako je t <0,6, mora se koristiti 2-D izraz brzine hlađenja, ali ako je t > 0,9, mora se upotrebiti 3-D izraz brzine hlađenja. Međutim, [2] utvrđeno je da ovaj kriterijum nije optimalan i modifikovan je tako da je korišćen 2-D izraz brzine hlađenja kada je vrednost τ manja od 1,5, a 3-D izraz brzine hlađenja je korišćen kada je τ bio veći od 2,0. Za vrednosti između ovih, razmotrene su prosečne vrednosti 2-D i 3-D hlađenja. Ova brzina hlađenja korišćena je kao jedan od ulaznih parametara za predviđanje FN u modelu Oak Ridge Feritnog broja (ORFN). U ovom istraživanju, kriterijumi koje koristi [2] se primenjuju za izračunavanje stepena hlađenja, pošto se vrednosti FN dobijene eksperimentima mogu uporediti sa vrednostima predviđenim ORFN modelom.

3. Rezultati i diskusija

Na osnovu dobijenih rezultata proučavan je uticaj brzine hlađenja na FN. Na slici 2 prikazane su grafički podaci izmerenih FN-a prema brzini hlađenja izračunatoj za zavarene spojeve limova različite debljine.

Na slici 2 se vidi da se s povećanjem brzine hlađenja količina zadržanog delta-ferita smanjuje za zavarene spojeve na limovma debljine 0,7 mm, 0,9 mm, 1,5 mm i 2,0 mm. Lim debljine 2,4 mm nije pokazao takav trend, čiji je mogući razlog objašnjen u kasnijim odeljcima.

Parameter	Value
K(thermal conductivity)	0.28 W/cm-°C
ρC_p (density*specific heat)	4.6 J/cm^3-°C
T' (temperature at which cooling rate is calculated)	1450°C
T_0 (ambient temperature)	25°C

Table 4. *Values of constant parameters used to calculate the cooling rate of the welds*
Tabela 4. *Vrednosti konstantnih parametara za izračunavanje brzine hlađenja zavarenih spojeva*

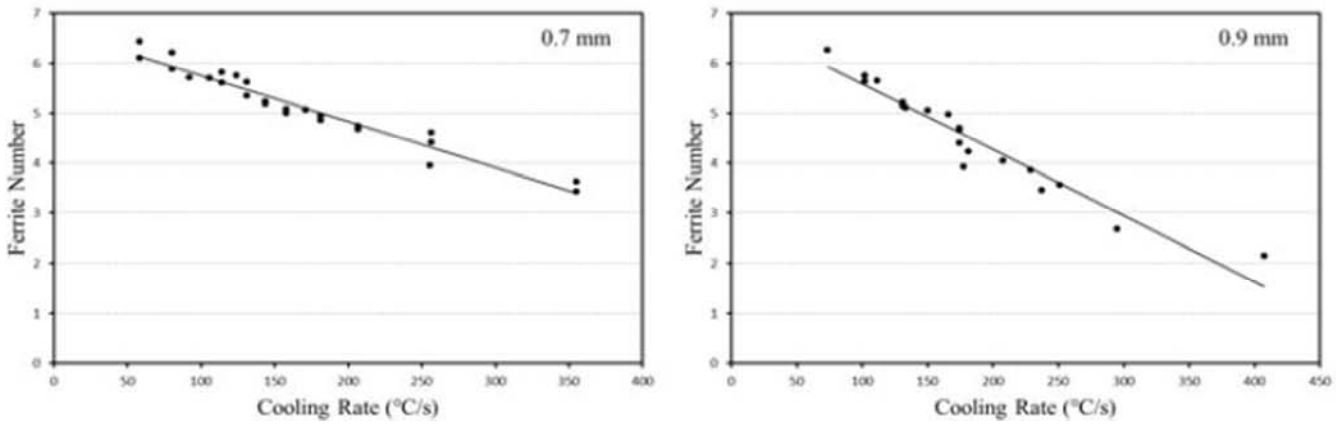

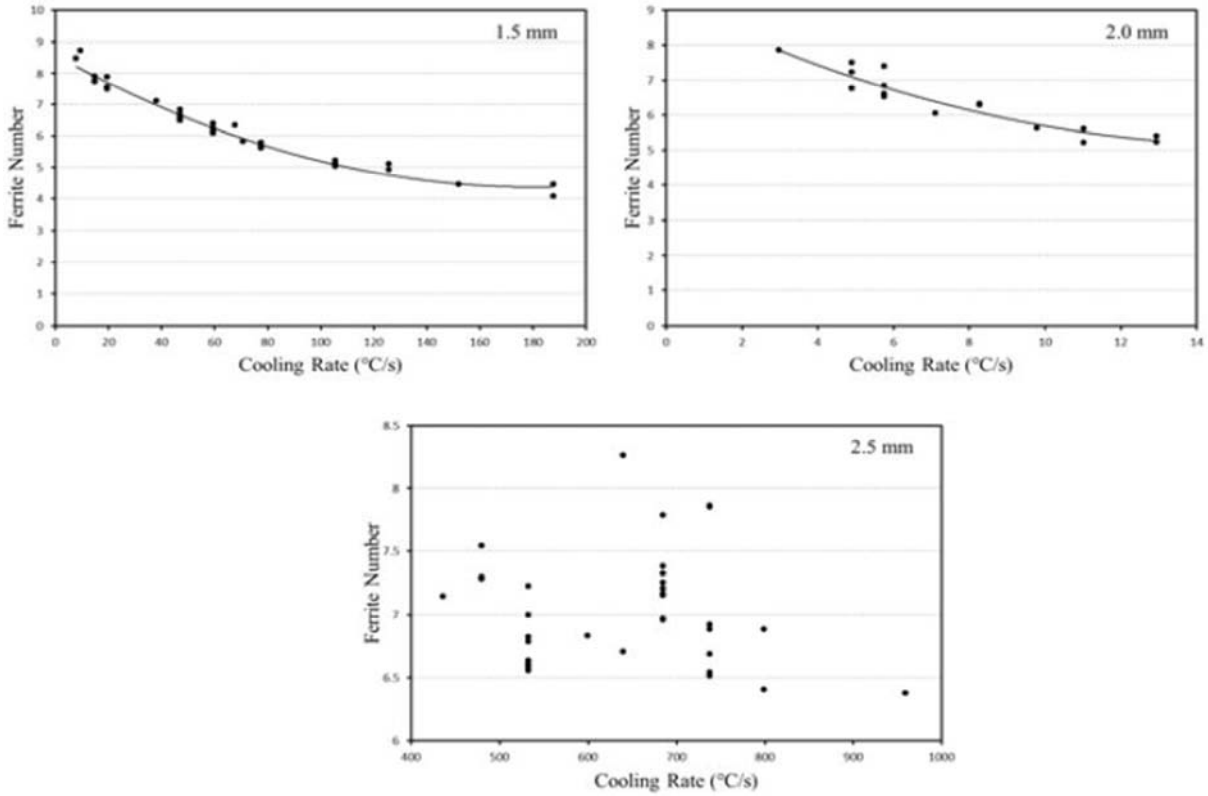

Figure 2. *Plots illustrating dependence of retained delta ferrite content on the cooling rate of the weld pool for various thickness sheets*

Slika 2. *Grafikoni koji prikazuju zavisnost sadržaja zaostalog delta ferita od brzine hlađenja zavarivačke kupke za limove različite debljine*

This reduction in retained delta-ferrite on increasing the cooling rate of the weld is in contradiction to what was expected. Considering the chemical composition of the sheet materials, and comparing the microstructures of the weld pool (shown in the later sections) to the microstructures shown in [4], it is evident that the weld pool has undergone an FA type of solidification. In this type of solidification, the weld pool primarily solidifies as delta-ferrite, following which a conversion to austenite takes place through a diffusion controlled reaction. In such cases, if the cooling rate is increased, the amount of residual delta-ferrite is expected to increase, owing to the fact that the conversion to austenite is supressed due to insufficient time available. The data in Figure 2 is plotted on a logarithmic scale of cooling rate in Figure 3. The curves for predicted FNs plotted against logarithms of cooling rates using the ORFN model developed by [2] using the chemistry of 0.7 mm and 0.9 mm thick sheets used for the experiments are shown in Figure 4. It can be clearly seen that for the experiments performed using the parameter ranges mentioned in Table 2, which lead to the logarithms of the cooling rates to vary between 1.70 and 2.60 for 0.7 mm and between 1.85 and 2.60 for 0.9 mm thick sheets, the FN must increase with increasing cooling rates.

Ovo smanjenje zaostalog delta-ferita povećanjem brzine hlađenja šava je u suprotnosti sa očekivanim. Uzimajući u obzir hemijski sastav materijala i upoređujući mikrostrukture kupki (prikazanih u kasnijim odeljcima) sa mikrostrukturama prikazanim u [4], očigledno je da je zavarivačka kupka podvrgnuta FA očvršćivanju. U ovoj vrsti očvršćavanja, zavarivačka kupka prvenstveno očvrsne kao delta-ferit, nakon čega se vrši konverzija u austenit reakcijom sa difuzionom kontrolom. U takvim slučajevima, ako se povećava brzina hlađenja, očekuje se da će se povećati količina preostalog delta-ferita zbog činjenice da je pretvaranje u austenit ugušeno zbog nedovoljnog raspoloživog vremena. Podaci na slici 2 prikazani su na logaritamskoj skali brzine hlađenja na slici 3. Krive za predviđene FN-e iscrtane prema logaritmima stepena hlađenja pomoću ORFN modela razvijenog od strane [2] koristeći hemiju limova debljine 0,7 mm i 0,9 mm za eksperimente prikazani su na slici 4. Jasno se može videti da za eksperimente izvedene korišćenjem raspona parametara navedenih u tabeli 2, koji dovode do toga da logaritmi brzina hlađenja variraju između 1,70 i 2,60 za 0,7 mm i između 1,85 i 2,60 za limove debljine 0,9 mm, FN mora da se povećava sa povećanjem brzine hlađenja.

-Kraj 1. dela NASTAVAK U SLEDEĆEM BROJU

ČASOPIS ZAVARIVANJE I ZAVARENE KONSTRUKCIJE

Cenovnik oglasnog prostora u četiri uzastopna broja 2019

	A4	2/2	1/1	1/2	1/4	1/8
	dimenzije (mm)	2 x 210 x 297	210 x 297	180 x 120	90 x 120	90 x 60
DIN	crno/beli	-	39 000	23 000	16 000	10 000
	kolor	105 000	75 000	-	-	-

- U cene nije uračunat PDV 20%.
- Objavljivanje oglasa u samo jednom broju iznosi 30% od datih cena.
- Reklamni tekstovi: 25 % od cene površine crno/belih oglasa.
- Dostava materijala:
  - za crno-beli film ili CD (Adobe Photoshop / CorelDRAW);
  - za kolor film ili CD (Adobe Photoshop / CorelDRAW);
  - izrada filma sa CD: 10 % od cene angažovanog prostora.
- Na web prezetaciji DUZS-a, (www.duzs.org.rs), na strani Marketing, objavljuje se pregled firmi-oglašivača sa podacima o glavnim grupama proizvoda/usluga i adresom web prezetacije. Svi posetioci naše web prezentacije mogu da posete i web prezentacije oglašivača, preko aktivnih linkova koji se nalaze na ovoj stranici!

WELDING & WELDED STRUCTURES, Quarterly review

Advertising prices for four successive numbers in 2019

	A4	2/2	1/1	1/2	1/4	1/8
	dimensions (mm)	2 x 210 x 297	210 x 297	180 x 120	90 x 120	90 x 60
EUR	black/white	-	840	432	336	240
	colour	2 640	1 680		-	-

- VAT 20% included.
- Advertising in one number only is 35% of the given prices.
- Commercial articles: 30 % of black/white advertising price.
- Print material:
  - for black/white CD (Adobe Photoshop / CorelDRAW)
  - for color CD (Adobe Photoshop / CorelDRAW).
- All the visitors of our web site may be linked to the advertisers' web site.

INDEKS OGLAŠIVAČA
ADVERTISERS INDEX

1. **ČLANARINA DUZS za 2019. godinu** …… **3.500 dinara**

   Članovima DUZS **GRATIS** godišnje izdanje časopisa "ZAVARIVANJE I ZAVARENE KONSTRUKCIJE"

2. **ČASOPIS "ZAVARIVANJE I ZAVARENE KONSTRUKCIJE" - 2019. godina**
   u slobodnoj prodaji (u cene je uračunat PDV 10%)**:**
   - cena pojedinačnog broja..... ……. 825 dinara
   - godišnja pretplata za 1 komplet brojeva godišnjeg izdanja…… 2.500 dinara
3. **ČASOPIS - stari brojevi** (u cene je uračunat PDV 10%)

   a) u slobodnoj prodaji:
   - cena pojedinačnog broja za 2017. godinu ..... …… 500 dinara
   - cena pojedinačnog broja za prethodne godine…….....…... 250 dinara

   b) beneficirane cene za članove DUZS:
   - cena pojedinačnog broja za 2018. godinu (pouzećem ili preuzimanjem) .....…….....…... 400 dinara
   - cena pojedinačnog broja za prethodne godine (pouzećem ili preuzimanjem) ……..... Gratis
4. **Knjiga Organizacija i ekonomika zavarivačkih radova –** autor: prof. dr Zoran Radojević (uračunat PDV 10%) ……. 1.045 dinara
5. **Zbirke standarda OBEZBEĐENJE KVALITETA U ZAVARIVANJU, komplet 4 toma** 6.750 dinara